

# Introduction

## Definitions

**Galaxy:** A mass condensation of order  $10^8 M_{\odot} - 10^{12} M_{\odot}$  composed of at least in part by stars and dust.  
A galaxy is held together by gravity.

**Protogalaxy:** A mass condensation like a galaxy, but devoid of stars. It is thought to be the stage before the galaxy.

Dark Matter: Missing/hidden matter.

A type of matter that is revealed only by its gravitational influence.

Dark matter candidates can be both baryonic and non-baryonic in nature.

Baryonic candidates are:

- MACHOs: Massive astrophysical compact halo objects. This includes planets, brown dwarves, compact stars, primordial black holes, neutron stars, faint old white dwarves, which are hard to detect.
- Cold molecular Hydrogen (traced by CO, C<sup>+</sup>, dust)
- Helium
- Low density ionized hydrogen (H<sup>+</sup>, e<sup>-</sup>)



The problem with baryonic candidates is that they can't explain all of the matter content of the Universe. The Big Bang could not have produced enough baryons and still be consistent with the observed elemental abundances.

Furthermore, separate observations of baryon acoustic oscillations, both in the CMB and large-scale structure of galaxies, set limits on the ratio of baryons to the total amount of matter. Those observations show that a large fraction of non-baryonic matter is necessary regardless of the presence or absence of MACHOs.

Non-baryonic candidates are:

- WIMPS: Weakly Interacting Massive Particles  
They are theorized to only interact via the weak force, don't have charges, and have masses in the order of  $100 \text{ GeV} \sim 100 m_p$
- Massive Neutrinos (as in neutrinos with non-zero mass. Today we assume that the leptonic neutrinos have masses  $\in [0.01, 0.7] \text{ eV}$ ,  
Note however that the massive neutrinos would constitute hot dark matter.
- Sterile neutrinos: Neutrinos that don't interact weakly (as opposed to 'active neutrinos', which are the usual neutrinos of the standard model)

The Big Bang is a good source for neutrinos creating  $400 \nu / \text{cm}^3$ .

- Axions: Very small, light, cold, hypothetical particles introduced to solve the strong-CP problem.

# Galaxy Evolution

The formation of a galaxy constitutes of the transformation of a proto-galaxy into a galaxy by initiating star formation.

During its lifetime, a galaxy can experience merging events with other galaxies, but a galaxy may also dislocate into several smaller galaxies. During these processes, the global parameters of a galaxy (total mass, size, energy, angular momentum...) transform. Dislocation however is a secular evolution, which means that the evolution proceeds over long time scales, meaning much longer than the rotational period (which is  $\sim 10^{7-8}$  yrs)





# Historical Development

## History of Galactic Astronomy

- 1609: Galileo Galilei: Discovering that the Milky Way is composed of stars
- 1658: Grassendi: Suggests that nebulae are made of stars, could be other milky ways
- 1750: Thomas Wright: Made several models of the Milky Way, either as a slab or a shell of stars
- 1755: Immanuel Kant: Intuitively, Kant understood that Gravity is scale-free. He attempted to consider Newtonian theories and facts. From observations of the planets orbiting the sun and satellites orbiting Jupiter and Saturn, he assumed that we have similar structures, but on different scales following a scale hierarchy, where the Milky Way was the upper version of the solar system.



His theory of the Milky Way included:

- the Milky Way is a rotating disk made of stars, kept in balance by Gravity

- Stars have a random velocity in addition to a general orientational motion

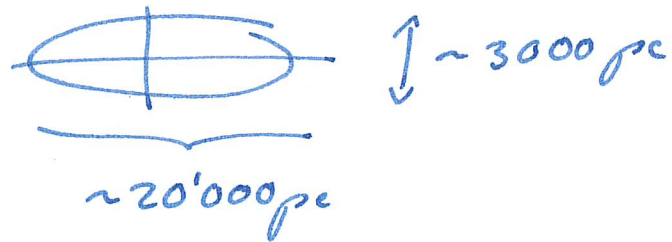
- The center of the Milky Way was not clear. (He assumed Sirius)

1761: Lambert: Made a hierarchical model of the Universe

1784-1790: William & Caroline Herschel: Created a catalogue of nebulae. Nebulae could be other Milky Way's, they are composed of stars, but they are also producing diffuse light, which they couldn't explain. Introduced the word "galaxy".

> 1845: Rosse: Discovers the spiral structure of some galaxies (nebulae)

~ 1900 - 1920: Kapteyn: Made different models of the "Universe" as the Milky Way with the sun at the center.  
Estimated size of the Milky Way:



~ 1928: Curtis and Shapley debate about the extra-galactic nature of spiral nebulae

- 1923: Hubble shows that M31 (Andromeda) is extra-galactic by measuring the distance / apparent magnitude of variable stars

1926: Lindblad: Discovers the differential rotation of the Milky Way as proposed by Kant:  
angular speed  $\Omega = \Omega(R)$  with  $\frac{d\Omega}{dR} < 0$

We see approximately the same number of stars in any given direction, at least by eye. Before  $\sim 1920$ , dust was ignored, and therefore many stars whose light was absorbed were missed.

## History of Cosmology

1755: Kant: Assumes that the initial Universe is static, uniform, and is composed of gas. Fluctuations and gravity lead to contractions from which the structures form.

A known problem with an initially static Universe is that no structures with angular momentum can form if there is no initial angular momentum, which would be the case for a static Universe.



1796: Laplace: Explains the formation of the solar system as the collapse of gas that has angular momentum into a rotating disk

1913: Poincaré: Still thinks in terms of the solar system and objects to Kant's view because he's thinking at the scale of the solar system

1915: Cosmology by Einstein introducing General Relativity. Allows for models of the entire Universe. At that time, it wasn't clear for astronomers whether the Milky Way was the entire Universe or whether there is more. With GR, they imagined expanding stars, not galaxies. (Hubble showed that M31 is outside the Milky Way only in 1926).

At first, Einstein assumed static models. Friedmann added expanding models which may be time dependent.

(At this point, we switch from the origin of the Universe, cosmogony, to the origin and evolution of the Universe, cosmology.)

~1929: Lemaitre & Hubble: Attribute galaxy redshift to the expansion of the Universe.

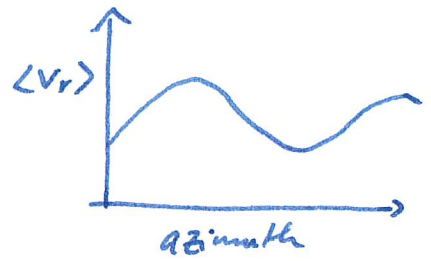
At this point, the Universe starts to consist of galaxies.

Only low redshift galaxies could be measured;  $z \approx 1$  came only ~1980. You could actually see the reddening of the higher redshift galaxies by eye.



# History of our EM-measurements of the Milky Way

1926: B. Lindblad measured the differential rotation of the nearby stars in the MW disk. By measuring the velocity via redshift of nearby stars and averaging over all, he obtained the relative movement and showed that it is consistent with movement on a disk.



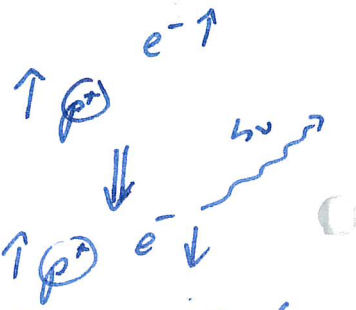
1932: Oort measured  $\sigma^2$  of the Milky Way and deduced that there was matter missing.

1933: Zwicky measured  $\sigma^2$  of galaxy clusters and deduced that there was matter missing.

At this point, dark matter was thought to be dust.

>1940: Opening of the electromagnetic spectrum, mostly through military advancement. This is the start of electro-magnetic observation and radio-astronomy.

1950: Discovery of the 21 cm emission line of atomic hydrogen. This line can't be observed in a laboratory: In the lab, the gas is too dense to measure the line correctly, but decreasing the density leads to hydrogen forming molecules.

The 21 cm line of atomic hydrogen comes from flipping  $\uparrow p$   $e^- \uparrow$  into the parallel spin of the electron into the antiparallel direction w.r.t. the proton. The diagram illustrates the spin configuration of a hydrogen atom. At the top, a proton (p) and an electron (e-) both have their spins pointing upwards, represented by upward-pointing arrows. A double-headed arrow between them indicates a parallel spin state. A downward arrow points to a second configuration where the proton's spin is still up, but the electron's spin is now pointing downwards, representing an antiparallel spin state. A wavy arrow labeled 'hv' points away from the electron, indicating the emission of a photon during the transition from the parallel to the antiparallel state.

The antiparallel configuration has a lower energy configuration because of the magnetic dipole of the two charged particles.

This transition was analytically predicted, but was not measurable in the lab.

This wavelength falls within the microwave region of the electromagnetic spectrum and these radio waves can penetrate through large clouds of cosmic dust that are opaque to visible light.

A substantial/sizeable amount of mass was discovered in the form of diffused hydrogen (interstellar gas).

> 1970: CO (1→0) transition with  $\lambda \sim 2.6 \text{ mm}$

The CO(1→0) emission line comes from a rotational transition. It stems from the fact that a CO molecule is asymmetric, which leads to dipolar emissions when rotating. Because  $\text{H}_2$  and  $\text{He}_2$  are symmetric, they don't have rotational transition lines.



Below 100K, there are good conditions for this transition. In these cold, "dense" ( $10^4 - 10^6 \text{ H}_2/\text{cm}^3$ ) regions, CO is an important tracer which led to the discovery of giant molecular clouds and a substantial amount of gas.

How can we estimate the  $\text{H}_2$  abundance from CO?

First, by measuring the velocity dispersion  $\sigma^2$  of CO emission in the cloud and assuming that the rest of the mass is made up from  $\text{H}_2$ . This revealed a relation that  $M(\text{H}_2) \propto I(\text{CO}(1 \rightarrow 0))$ .

We can also compare with emissions from other molecules, like  $\text{HCO}$ ,  $^{12}\text{C}^{16}\text{O}$ ,  $^{13}\text{C}^{18}\text{O}$ ,  $\text{HCN}$ ,  $\text{C}^+$ , cold dust.

However, these other tracers are less abundant.

> 1980: Detecting X-rays by satellites  
(it needs to be done outside the atmosphere, because the atmosphere absorbs X-rays.)

Also Infrared satellites allow for infrared observations. Since the earth is a hot body with  $\sim 300\text{K}$ , it radiates a lot, making infrared hard to observe from the ground.

It was found that dust is emitting infrared radiation, at wavelengths  $\sim 10-20\mu\text{m}$  for "warm" dust and  $\sim 50-800\mu\text{m}$  for cold dust.

The coldest observable dust is still a frontier, as very cold dust  $< 10\text{K}$  barely emits anything.

Since about 1980, galaxy catalogues are vastly improved and showed that galaxies are not randomly distributed, but form large scale structures. Through simulations it was confirmed that galaxies form in a hierarchical way, not via spherical monolithic collapse.



## Other Observations and Measurements

> 1990: Detection of high-energy neutrinos  
(as opposed to low-energy neutrinos  
created  $\sim 1s$  after the big bang  
and heavily redshifted until today)

> 2015: Gravitational Waves

## Development of Computer Simulations

> 1960: First computer simulations. Extension of  
the mathematical tools to set up models.  
They started out with 200 body  
models for galaxy simulations (like  
collisions, disks...)

$\sim 1970$ :  $10^5$  body simulations

$\sim 1980$ : Also introducing gas physics

$\sim 2010$ :  $10^{10}$  body simulations

# Multiwavelength View of the Milky Way

## Wavelength overview

	$\nu$	$\lambda$	$E$
Radio Continuum	MHz - GHz	cm - m	$\sim \mu\text{eV}$
H hyperfine emission	1.42 GHz	21cm	5.9 $\mu\text{eV}$
CO emission	115 GHz	2.6mm	480 $\mu\text{eV}$
Far infrared	3-25 THz	12, 60, 100 $\mu\text{m}$	0.012 - 0.1 eV
Mid infrared	28-44 THz	6.8 - 10.8 $\mu\text{m}$	0.11 - 0.18 eV
Near infrared	86-240 THz	1, 25 - 7.5 $\mu\text{m}$	0.35 - 1 eV
Visible	500 - 700 THz	0.4 - 0.6 $\mu\text{m}$	2 - 3 eV
UV	$\sim 10$ PHz	10 - 100 nm	$\sim 10$ eV
X - Rays	60 - 360 PHz	0.8 - 5 nm	1.5 keV
$\Gamma$ - Rays	$> 72$ EHz	$10^{-15}$ m	$> 300$ MeV

## Radio Continuum @ 408 MHz

This type of radiation is caused by accelerated electrons. The physical processes behind it can be:

- Synchrotron emission: Acceleration due to a present magnetic field.

⇒ There is a galactic magnetic field in the MW in the order of  $\mu\text{G}$ . Its origin is still unclear, but most likely it's due to a turbulent hot charged medium, giving the dynamo effect.

- free-free emissions: Electrons scattering off ions without being captured.

(also called thermal bremsstrahlung.)

The acceleration is due to the present electric field of the plasma where ions and electrons can scatter off each other without capture

⇒ There is a hot plasma  $T > 10^4 \text{ K}$  present. Below  $10^4 \text{ K}$ , hydrogen isn't ionized and we won't have electron emissions.

- Point Sources: Some point sources can be seen, which are very bright.  
This is hot plasma in supernova remnants.

The general structure revealed by the radio continuum waves at 408 MHz is:

- Intense signal near the center  
↳ a lot of hot plasma there
- The distribution is smooth
- There is some sources in the disk, revealing that the disk is not really flat
- A couple of SN remnants as bright point sources can be seen,



## H-hyperfine emission @ 1.42 GHz

This is the 21 cm emission line of atomic, neutral hydrogen (HI). The emission line stems from flipping the initially parallel spin of electron and proton to the antiparallel case, which is energetically favourable because of the magnetic dipole of the particles.

The 21 cm line traces the "cold" and "warm" atomic hydrogen with  $T \lesssim 10^3$  K. The hydrogen can be found in the atomic state because it is very diffuse, the density is too low to efficiently form molecular hydrogen, which requires a 3-body collision.

Around the center of the galaxy, the hydrogen distribution is very thin. Why? Because the gravitational potential around the center of the galaxy heats the gas, and the density increases, thus removing diffuse hydrogen to make hot plasma out of it, which we see in the 1.42 GHz radio continuum.



## Radio Continuum @ 2.5 GHz

Traces mostly synchrotron radiation of electrons being accelerated by present magnetic fields.

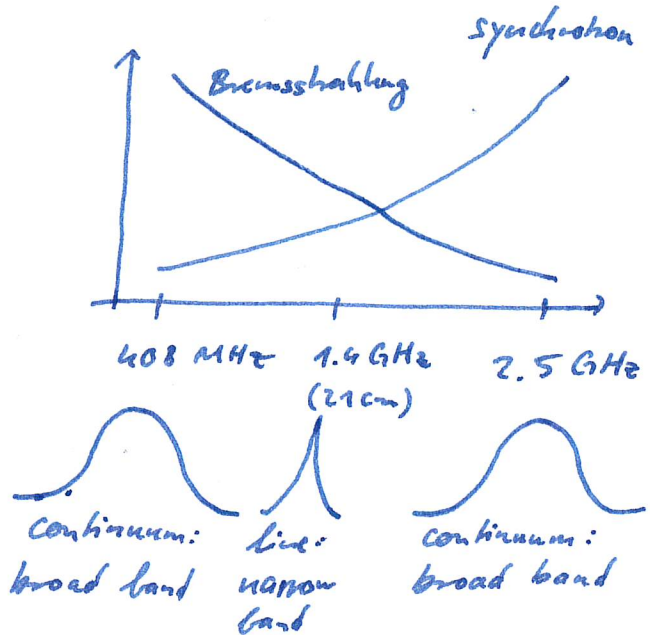
This radiation again traces hot plasma, in which one can find free electrons.

There is a lot of overlap with the 408 MHz radiation.

The radio continua are measured in broad band spectra, which typically have widths of  $\sim 100$  MHz.

With increasing frequency, the radiation contribution of Bremsstrahlung decreases, while synchrotron radiation increases.

Thus measuring the radio continua around different peak wavelengths/frequencies helps distinguish between these two radiation sources.



Synchrotron radiation also traces the galactic magnetic field. Close to the center, the magnetic field is like a pole. In the disk, it is circulating along the disk, but has turbulences.

The polarisation of the radiation can give us the orientation of the magnetic field, however only integrated along the line of sight.

Another option for obtaining the information of the directionality of the magnetic field is the line splitting due to the Zeeman effect.

## CO emission @ 115 GHz

The CO(1 $\rightarrow$ 0) emission line @ 2.6mm is a rotational transition line. It stems from the fact that a CO molecule is asymmetric, which leads to dipolar emissions when rotating. (H<sub>2</sub>, He<sub>2</sub> are symmetric, thus they don't have rotational lines). [Is in microwave range.]

Below 100K, there are good conditions for this transition, but CO freezes at  $\approx$  20K, giving a lower temperature limit for the observed clouds.

It also traces only dense clouds, up to  $n_{\text{H}_2} \sim 10^5 \text{ cm}^{-3}$ , at which point CO becomes opaque, and not below  $n_{\text{H}_2} \approx 10^2 \text{ cm}^{-3}$ , at which point the CO molecules can be destroyed.

The H<sub>2</sub> and He<sub>2</sub> abundances are estimated by assuming that most of the mass of the cloud is made up from these molecules and measuring the velocity dispersion from the CO emission.



Another problem is that the CO/H<sub>2</sub> abundance relation is not universal, and since C and O needs to be produced in a star, CO is not a good tracer in regions with no stars.

Since CO traces cold, dense molecular clouds, it was the first evidence for molecular clouds in our galaxy.

It also showed that molecular clouds are not round at all, but fractional.

Subclumps are inside subclumps over 4 orders of magnitude differences in size.

The hierarchical composition can be seen in the image. The high/tall clouds close to the center in the image aren't close to the center at all, but close to us, which makes them look tall.

## Far IR radiation

Thermal emission of cold dust which have been warmed up by stars.

## Mid IR radiation

Emitted by PAH (polycyclic aromatic hydrocarbons) molecules, which are complex molecules, commonly found around red giant stars or during star formation regions.

## Near IR radiation

Reveals cold stars ( $T \sim 3000 \text{ K}$ ) in the bulge, bar, disk, which are hidden in the visible spectrum. Most of the mass is detected in these kinds of maps, since a large fraction of stars are small and cold.

## Visible Spectrum

The absorption due to the present dust is visible. The dust clouds have sharp edges.

## Ultraviolet Radiation

There is almost no information in UV for the galaxy as a whole. The image mostly looks like a diffuse fog because of strong absorption/diffusion due to H and H<sub>2</sub>.

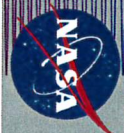
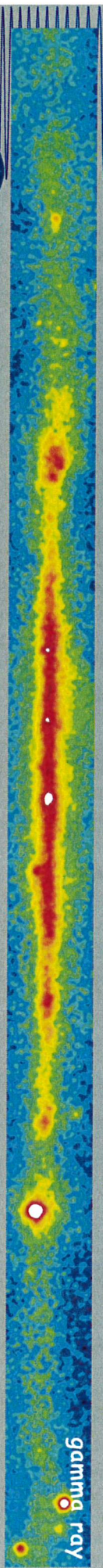
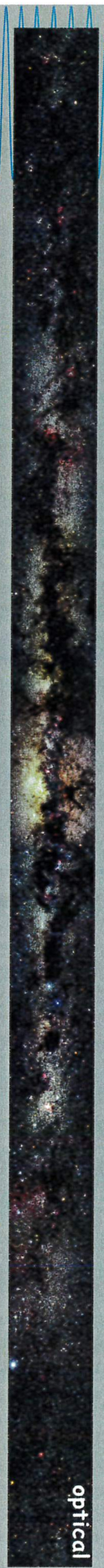
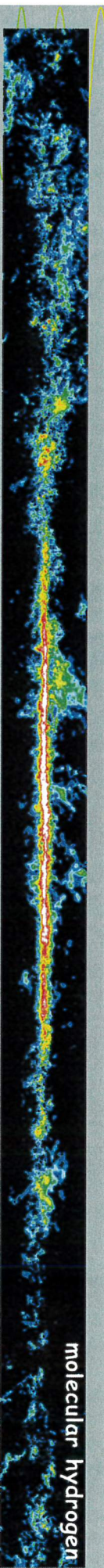
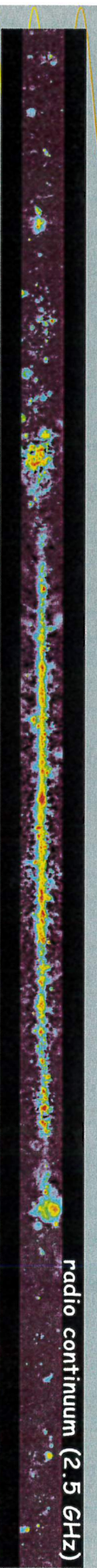
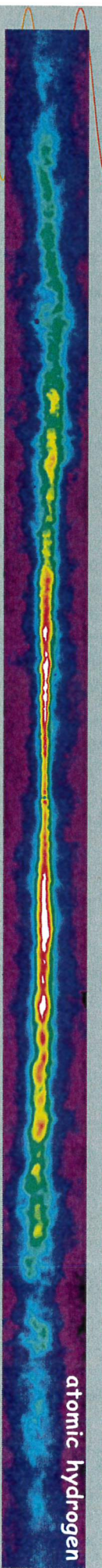
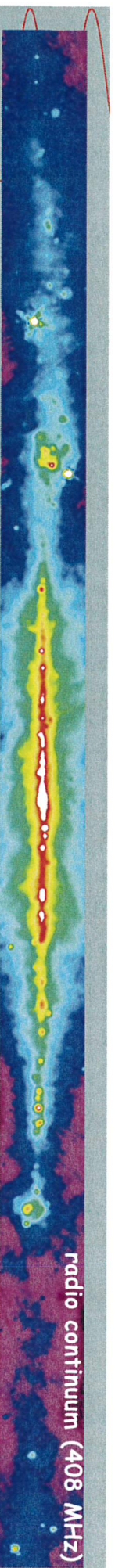
## X-Rays

Traces very hot ( $10^5 - 10^6$  K) medium. The blue point sources are supernova remnants.

## $\Gamma$ -Rays

It is very rare. Point sources are SN remnants or pulsars, the diffuse emission comes from cosmic rays interacting with the gas, thus increasing





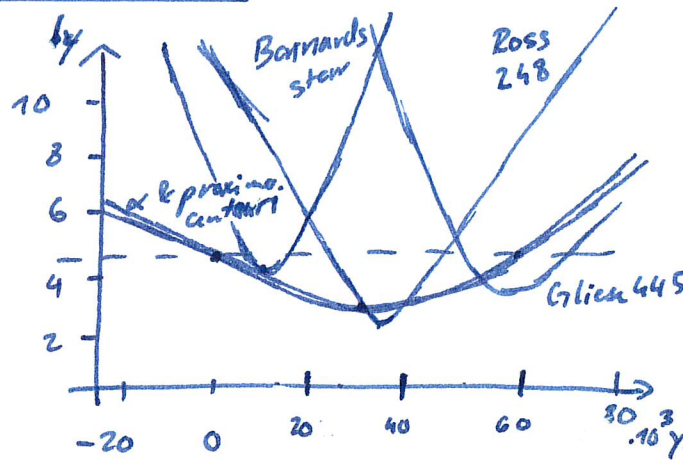
# Multiwavelength Milky Way





# The Solar Neighbourhood

The closest star to the sun is changing over time.



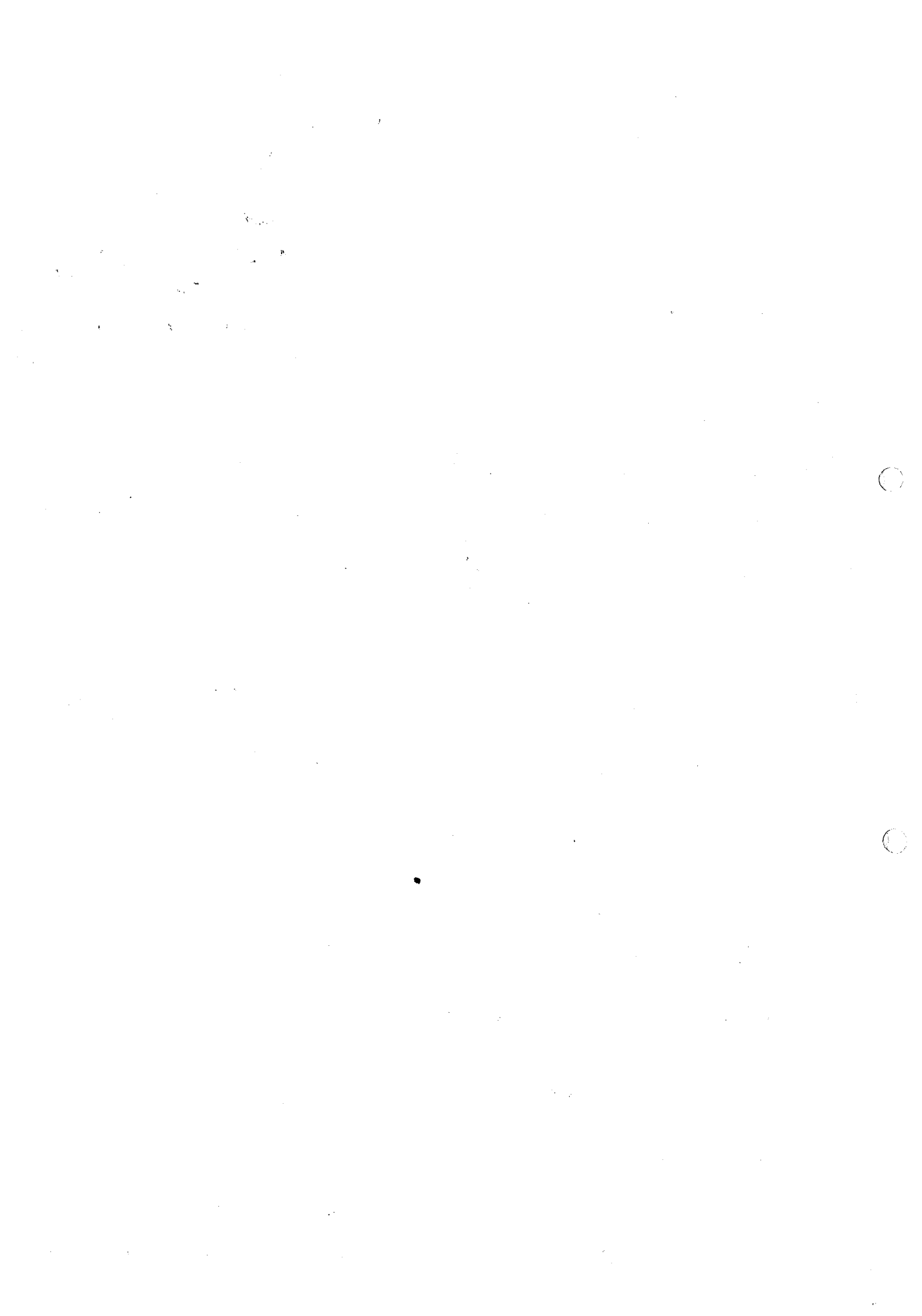
No star could have crossed the solar system, since the outer heavy planets don't have strongly elliptical orbits, but they all have eccentricity  $\ll 1$ .

Nearby stars up to 1 kpc are visible by eye. They show a random distribution and random motion.

The sun is currently passing through a local gas cloud (on a pc scale.)

On a 100-1000 pc scale, the sun is in a hot, diffuse bubble, probably stemming from a supernova  $3 \cdot 10^5$  years ago, which resulted in the Trumpler neutron star 800 ly from the sun.





# Local Stellar Kinematics

## Available Data

The data available from other stars is:

- position on the sky  $(l, b)$   
in galactic coordinates
  - distances of stars using the parallax method
- } give 3D cartesian coordinates
- radial velocity of stars through the doppler effect (spectrometry)
  - angular velocity ("proper motion") on the sky. Together with the distance, this gives the tangential velocity.

From these data, we can derive a handful of statistical properties.

## Local Standard of Rest

We can define the LSR, which is the reference frame set by the sample of stars that we work with. The idea is to estimate the local velocity as the average velocity of nearby stars.

- We expect that the average velocity of a big enough sample (which is comoving in the galaxy) should be zero.
- We measure the velocities of this group of stars and obtain the average velocity  $\langle \vec{v} \rangle$ , which is non-zero.
- Attribute this non-zero average velocity to the peculiar velocity of the sun. In this case, the actual peculiar velocity of the sun is  $\vec{v}_0 = -\langle \vec{v} \rangle$  [such that if you move all stars' velocities into the rest frame of the sun, we get  $\langle \vec{v} \rangle|_{\text{Frame of Sun}} = 0$ ].  
-  $\frac{\langle \vec{v} \rangle}{|\langle \vec{v} \rangle|}$  is then the "apex", the direction of the sun's motion and  $\frac{\langle \vec{v} \rangle}{|\langle \vec{v} \rangle|}$  is the antapex.



## Determining $\vec{v}_0$ by Least-Squares

Here for radial velocities. A closely analogous procedure works for proper motion data.

Let:  $\vec{v}_k$  : Velocity of  $k$ -th star  
 $\hat{x}_k$  : Unit vector pointing to  $k$ -th star

Then:  $\hat{x}_k \cdot \vec{v}_k$  is the radial velocity of the  $k$ -th star in the reference frame of the sun. Moving to a LSR, we have  $\vec{v}_0 \neq 0$  and

$$\hat{x}_k \cdot \vec{v}_k = \hat{x}_k \cdot \vec{v}_0 + v_r \quad (k=1, \dots, N)$$

when we assume that  $N$  stars have been observed.

These equations have infinitely many solutions, since if  $\vec{v}_k$  and  $\vec{v}_0$  solve them, so do  $\vec{v}'_k \equiv \vec{v}_k + \vec{v}$  and  $\vec{v}'_0 \equiv \vec{v}_0 + \vec{v}$ , which is a simple boost in the reference frame.

To pick out the solution of interest, we have to impose the condition that the  $\vec{v}_k$  have zero mean. Suppose that this condition is satisfied in the unprimed frame. Then the following quantity simplifies:

$$\begin{aligned}
 \sum_k (\hat{x}_k \cdot \vec{v}_k')^2 &= \sum_k (\hat{x}_k \cdot (\vec{v}_k + \vec{v}))^2 = \sum_k (\hat{x}_k \cdot \vec{v}_k + \hat{x}_k \cdot \vec{v})^2 \\
 &= \sum_k \left[ (\hat{x}_k \cdot \vec{v}_k)^2 + (\hat{x}_k \cdot \vec{v})^2 + 2 \underbrace{\hat{x}_k \cdot \hat{x}_k}_{=1, \text{ are unit vectors}} \cdot \vec{v} \cdot \vec{v}_k \right] \\
 &= \sum_k \left[ (\hat{x}_k \cdot \vec{v}_k)^2 + (\hat{x}_k \cdot \vec{v})^2 \right] + 2 \vec{v} \cdot \underbrace{\sum_k \vec{v}_k}_{=N \langle \vec{v}_k \rangle = 0} \\
 &= \sum_k \left[ (\hat{x}_k \cdot \vec{v}_k)^2 + (\hat{x}_k \cdot \vec{v})^2 \right]
 \end{aligned}$$

Using this, it is easy to see that

$$S \equiv \sum_k (\hat{x}_k \cdot \vec{v}_k')^2 = \sum_k (\hat{x}_k \cdot \vec{v}_k)^2 + \sum_k (\hat{x}_k \cdot \vec{v})^2 > \sum_k (\hat{x}_k \cdot \vec{v}_k)^2$$

It follows that the desired frame is that which minimizes  $S$ .

## Dynamical standard of rest

(Binney & Merifield §10.3.3)

The "solar neighbourhood" must be considered to be a sphere large enough to contain an adequate sample of whatever stars are under investigation. If these stars are intrinsically rare (e.g. most kinds of giants) the sphere may have to have a non-negligible radius compared to the size of the Milky Way and the effects within it of differential rotation may be significant.

Assuming that the Milky Way is axisymmetric, a formula can be derived for the rotation speed  $v_R(R)$ , which defines the frame for the dynamical standard of rest, using an expression for the force from the axisymmetric potential and the centrifugal force.



The dynamical local standard of rest is then defined as the frame which has the current velocity of a fictional particle that moves around the plane of the Milky Way on the closed circular orbit that passes through the present location of the sun.

The condition for a circular orbit is

$$\frac{v^2}{R} = - \frac{\partial \Phi}{\partial R} (R, z=0)$$

The constants of motion are the

Energy

$$E = \frac{1}{2} \dot{\vec{v}}^2 + \Phi(R, z)$$

Angular Momentum

$$L = \vec{R} \times \vec{v}$$

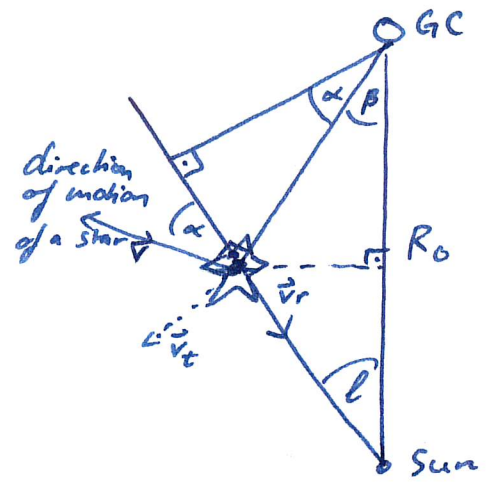
The sun rotates clockwise around the MW center with the rotation period of about 200 million yrs with a velocity of  $\sim 220 \text{ km s}^{-1}$  at a radius  $r_0 \sim 8 \text{ kpc}$ .

The Sun's peculiar velocities have been measured to be  $(U, V, W)_0 \cong (11, 12, 7) \text{ km s}^{-1}$ .

(Schönrich, Binney, Dehnen 2009)

# Galactic Rotation, Kinematics of differential rotation

We can define the local standard of rest (LSR) as the point in space at the Sun's galactocentric distance that is moving on a perfectly circular orbit around the center of the galaxy, and use it as the frame of reference to define the velocities of stars relative to this frame.



The Sun's velocity relative to this frame is called the 'solar motion', other stars' velocities are their 'peculiar velocities'.

We can measure (other) star's velocities by

- measuring radial velocity via doppler shifts
- measuring tangential velocities via proper (angular) velocities on the sky and the distance to the star

Then, following the sketch on the previous page.

$$v_r = V \cos \alpha$$

$$v_t = V \sin \alpha$$

and the local standard of rest velocities

$$v_{r,0} = v_0 \sin l$$

$$v_{t,0} = v_0 \cos l$$

where  $\vec{v}_0$  is the LSR velocity at  $R_0 = R_\odot$   
giving us the observed velocities

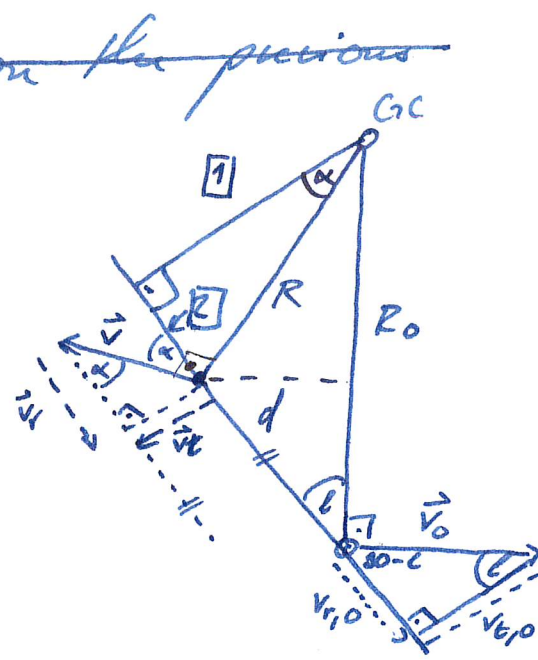
$$v_R = v_r - v_{r,0} = V \cos \alpha - v_0 \sin l$$

$$v_T = v_t - v_{t,0} = V \sin \alpha - v_0 \cos l$$

If we also assume that the other star is moving along a circular orbit, we can write:

$$\boxed{1} \quad R \cos \alpha = R_0 \sin l$$

$$\boxed{2} \quad R \sin \alpha = R_0 \cos l - d$$





Then let us substitute

$$\Omega(R) \equiv \frac{V(R)}{R} \quad \text{angular velocity}$$

into the equations:

$$V_R = V \cos \alpha - V_0 \sin l$$

$$= \frac{V}{R} \cdot R \cos \alpha - \frac{V_0}{R_0} R_0 \sin l$$

$$= \Omega R_0 \sin l - \Omega_0 R_0 \sin l = \boxed{(\Omega - \Omega_0) R_0 \sin l}$$

$$V_T = V \sin \alpha - V_0 \cos l = \frac{V}{R} R \sin \alpha - \frac{V_0}{R_0} R_0 \cos l$$

$$= \Omega (R_0 \cos l - d) - \Omega_0 R_0 \cos l$$

$$= \boxed{(\Omega - \Omega_0) R_0 \cos l - \Omega d}$$

However,  $d$  is difficult to measure for stars that are far away. For nearby stars, we can use the parallax technique.

Then for nearby stars,  $d \ll R$ , and we can approximate using a Taylor expansion:

$$\Omega = \Omega_0 + \frac{d\Omega}{dR} \Big|_{R=R_0} \underbrace{(R-R_0)}_{=d} + \mathcal{O}(\underbrace{(R-R_0)^2}_{d^2})$$

$$\Rightarrow \Omega - \Omega_0 \approx \frac{d\Omega}{dR} \Big|_{R_0} (R - R_0)$$

$$= \frac{d}{dR} \left( \frac{v}{R} \right) \Big|_{R_0} (R - R_0) = \left[ \frac{1}{R^2} \frac{dv}{dR} \cdot R - \frac{1}{R^2} v \frac{dR}{dR} \right] \Big|_{R_0} (R - R_0)$$

$$= \left[ \frac{1}{R} \frac{dv}{dR} - \frac{v}{R^2} \right] \Big|_{R_0} (R - R_0)$$

Let us define the so-called 'Cort's constant'

A.

$$A = -\frac{1}{2} \left( R \frac{d\Omega}{dR} \right) \Big|_{R_0}$$

$$= \frac{1}{2} \left( \frac{v}{R} - \frac{dv}{dR} \right) \Big|_{R_0}$$

which gives

$$\Omega - \Omega_0 \approx \frac{1}{R} \left[ \frac{dv}{dR} - \frac{v}{R} \right] \Big|_{R_0} (R - R_0)$$

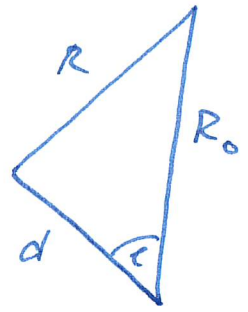
$$= -2A \frac{R - R_0}{R}$$

and

$$V_R = (\Omega - \Omega_0) R_0 \sin l = -2A (R - R_0) \frac{R_0}{R} \sin l$$

We once again simplify this expression.  
This time, we use the law of cosines:

$$R^2 = R_0^2 + d^2 - 2R_0 d \cos \ell$$
$$\approx R_0^2 - 2R_0 d \cos \ell \quad \text{for } d \ll R_0$$



$$\Rightarrow R^2 - R_0^2 \approx -2R_0 d \cos \ell$$

$$= (R - R_0) \underbrace{(R + R_0)}_{\approx 2R_0} \approx -2R_0 d \cos \ell$$

$$\Rightarrow (R - R_0) \approx -d \cos \ell$$

This gives us

$$V_R = -2A (R - R_0) \frac{R_0}{R} \sin \ell \approx +2A d \cos \ell \underbrace{\frac{R_0}{R} \sin \ell}_{\approx 1}$$
$$\approx Ad 2 \sin \ell \cos \ell = Ad \sin (2\ell)$$

$$\boxed{V_R = Ad \sin (2\ell)}$$



Similarly, we can derive (from the matter)

$$v_T = Ad \cos 2l + Bd$$

$$\text{where } B \equiv - \left( \Omega + \frac{1}{2} R \frac{d\Omega_z}{dR} \right) \Big|_{R_0}$$
$$= - \frac{1}{2} \left( \frac{v}{R} + \frac{dv}{dR} \right) \Big|_{R_0}$$

is another Oort's constant.

$\Omega_z$  is the  $z$ -component of the angular rotation vector  $\vec{\Omega}$ . Because the Milky Way rotates clockwise, we have

$$\Omega_z = -\Omega.$$

Physical interpretation of A and B:

- A measures the shear\* in the disk at the position of the sun.

Since  $A \equiv -\frac{1}{2} \left( R \frac{d\Omega}{dR} \right) \Big|_{R_0}$ , it would be zero if the rotation is independent of the radius, i.e.  $\frac{d\Omega}{dR} = 0$ , which would be the case for a solid body.

\* Shear as in deviation from rigid motion.

- $B$  measures the vorticity of the material of the disk, i.e. its tendency to circulate about any given point. It is also a measure of the angular momentum gradient.

Since  $A = +\frac{1}{2} \left( \frac{v}{R} - \frac{dv}{dR} \right) \Big|_{R_0}$

and  $B = -\frac{1}{2} \left( \frac{v}{R} + \frac{dv}{dR} \right) \Big|_{R_0}$

it immediately follows that

$$v = R_0 (A - B)$$

$$\frac{dv}{dR} \Big|_{R_0} = -(A + B)$$

Typically, for spiral galaxies the circular velocity curves are flat or mildly rising at high radii. So if the Milky Way's circular speed curve followed this pattern, we would expect

$$\frac{dv}{dR} \Big|_{R_0} = -(A + B) \geq 0 \Rightarrow A + B \leq 0$$





# Oort's Constants

We already introduced earlier the "classical" Oort Constants

$$A = +\frac{1}{2} \left( \frac{v}{R} - \frac{dv}{dR} \right) \Big|_{R_0} = -\frac{1}{2} \left( R \frac{d\Omega}{dR} \right) \Big|_{R_0}$$

$$B = -\frac{1}{2} \left( \frac{v}{R} + \frac{dv}{dR} \right) \Big|_{R_0} = - \left( \Omega + \frac{1}{2} R \frac{d\Omega}{dR} \right) \Big|_{R_0}$$

There is however a more general way to define them.

$$\text{Let } \delta \vec{v}(x) \equiv \vec{v}(\vec{x}) - \vec{v}_{\text{LSR}}$$

Then, for stars close to the Sun, we expand:

$$\vec{v}(\vec{x}) = \vec{v}_{\text{LSR}}(\vec{x}) + (\vec{x} - \vec{x}_{\text{LSR}}) \frac{\partial \vec{v}}{\partial \vec{x}} + \mathcal{O}[(\vec{x} - \vec{x}_{\text{LSR}})^2]$$

$$\Rightarrow \delta \vec{v}(x) = \vec{v}(\vec{x}) - \vec{v}_{\text{LSR}} \approx (\vec{x} - \vec{x}_{\text{LSR}}) \frac{\partial \vec{v}}{\partial \vec{x}}$$

We define the coordinate system such that the  $x$ -component points toward the galactic center and the  $y$ -component along the MW's rotation:



Now rewrite the matrix  $\frac{\partial \vec{v}}{\partial \vec{x}}$  as

$$\frac{\partial \vec{v}}{\partial \vec{x}} \equiv \begin{pmatrix} k+c & a-b \\ a+b & k-c \end{pmatrix}$$

Such that

$$\begin{pmatrix} \delta v_x \\ \delta v_y \end{pmatrix} = \begin{pmatrix} k+c & a-b \\ a+b & k-c \end{pmatrix} \begin{pmatrix} x \\ y \end{pmatrix} = \begin{pmatrix} (k+c)x + (a-b)y \\ (a+b)x + (k-c)y \end{pmatrix}$$

where we set  $\vec{x}_{LSR} \equiv 0$ .

We would then expect the mean radial velocity of the stars at  $\vec{x} = (x, y)$  to be

$$v_r = \frac{1}{d} \vec{x} \cdot \delta \vec{v} = \frac{\vec{x} \cdot \delta \vec{v}}{|\vec{x} - \vec{x}_{LSR}|}$$

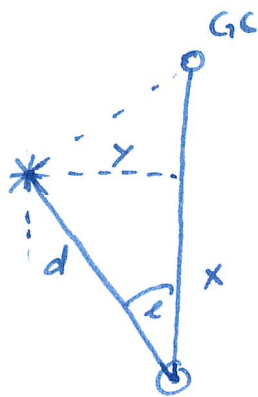
projection of velocity difference  
along unit vector in direction  
of the star at  $\vec{x}$

$$\begin{aligned} &\approx \frac{1}{d} \left[ (k+c)x^2 + (a-b)yx + (a+b)xy + (k-c)y^2 \right] \\ &= \frac{1}{d} \left[ (k+c)x^2 + (k-c)y^2 + 2axy \right] \end{aligned}$$

In terms of galactic latitude,  
we have

$$x = d \cos l$$

$$y = d \sin l$$



giving us

$$v_r = \frac{1}{d} \left[ (k+c)d^2 \cos^2 l + (k-c)d^2 \sin^2 l + 2ad^2 \cos l \sin l \right]$$

$$= d \left[ k(\sin^2 l + \cos^2 l) + c(\cos^2 l - \sin^2 l) + 2a \sin l \cos l \right]$$

$$= d \left[ k + c \cdot \cos 2l + a \sin 2l \right] \quad \left( + O(d^2) \right) \\ \text{from the start}$$

$\Rightarrow$  we could determine  $a$ ,  $c$ , and  $k$  by  
measuring radial velocities.

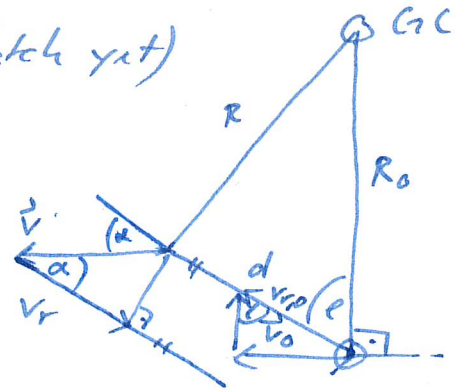
Similarly, if we derive this equation for the  
proper motions, we could determine  $b$ ,  $c$  and  $k$   
by measuring the proper motions.



If we now assume circular motions in a disk; (not assumed in this sketch yet)

$$v_r = v \cos \alpha, \quad v_{r,0} = v_0 \sin l$$

$$\Rightarrow v_R = v_r - v_{r,0} = v \cos \alpha - v_0 \sin l$$

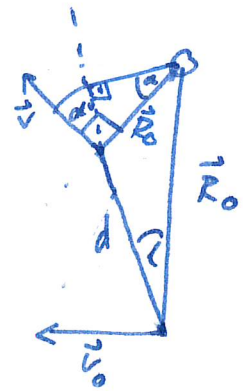


For circular motion, we also have

$$\vec{v} \perp \vec{R}, \quad \vec{v}_0 \perp \vec{R}_0$$

$$\Rightarrow R \cos \alpha = R_0 \sin l$$

$$R \sin \alpha = R_0 \cos l - d$$



and furthermore substituting

$$\Omega(R) = \frac{v(R)}{R}$$

gives

$$v_R = v \cos \alpha - v_0 \sin l = \frac{v}{R} R \cos \alpha - \frac{v_0}{R_0} R_0 \sin l$$

$$= \Omega R_0 \sin l - \Omega_0 R_0 \sin l$$

$$= (\Omega - \Omega_0) R_0 \sin l$$

$$\approx \left( \Omega_0 + \left. \frac{d\Omega}{dR} \right|_{R_0} (R - R_0) + \mathcal{O}[(R - R_0)^2] \right) - \Omega_0) R_0 \sin l$$

$$\approx \left. \frac{d\Omega}{dR} \right|_{R_0} (R - R_0) R_0 \sin l = -2A (R - R_0) \frac{R_0}{R} \sin l$$

And we're back where we started.

Comparing the expression for circular motion

$$v_R = -2A \underbrace{(R-R_0)}_{\equiv d} \underbrace{\frac{R_0}{R}}_{\approx 1} \sin \ell \approx Ad \sin 2\ell$$

↑  
see derivation in previous chapter

to the more general one

$$v_R = d[k + c \cos 2\ell + a \sin 2\ell]$$

we immediately see that for the circular rotation in the disk, we have

$$k=0, \quad c=0, \quad a=A$$

From proper motions, we also get  $b=B$ .

Measurements indeed show  $k \approx 0, c \approx 0,$

$$A \approx 14 \frac{\text{km/s}}{\text{kpc}}, \quad B \approx -12 \frac{\text{km/s}}{\text{kpc}}$$

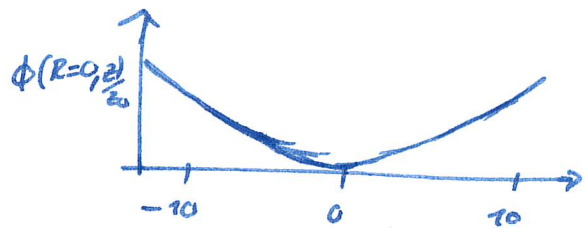
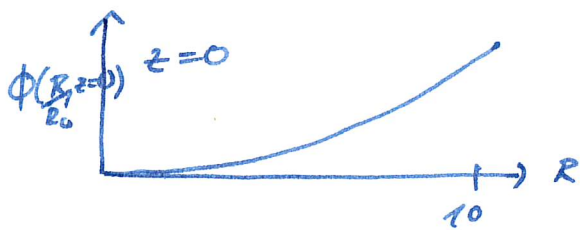




# Differential Velocity Study in a Rotating Disk

For a simple power law spheroidal and axisymmetric potential of the form

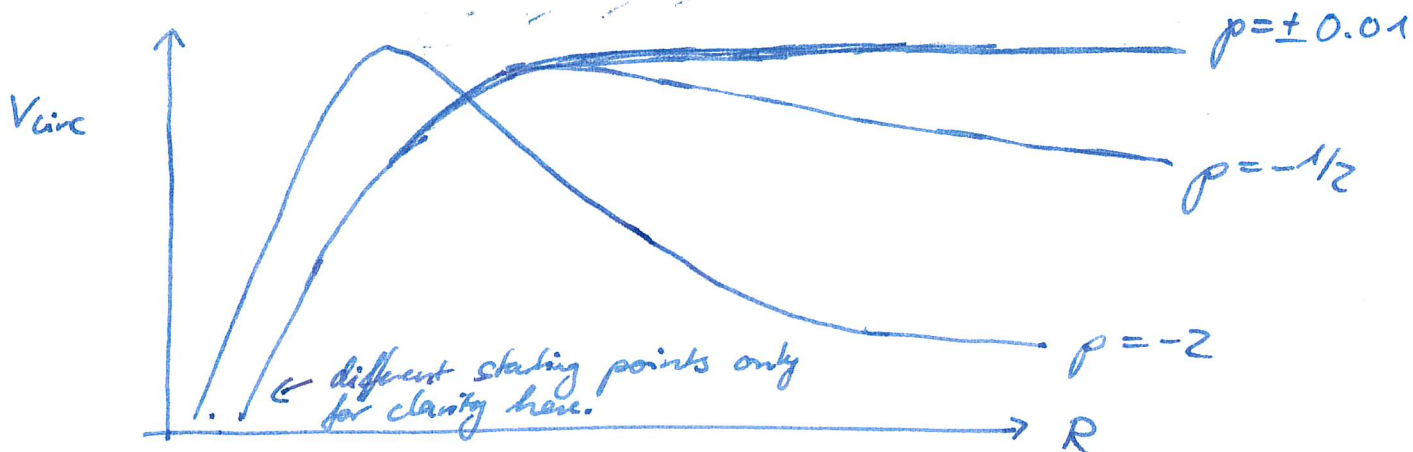
$$\Phi(R, z) = \frac{1}{\rho} \left[ 1 + \frac{R^2}{h^2} + \frac{z^2}{z_0^2} \right]^{1/2 \rho}$$



$$\text{Then } \left. \frac{\partial \Phi}{\partial R} \right|_{z=0} = \frac{R}{h^2} \left[ 1 + \frac{R^2}{h^2} \right]^{\frac{\rho-2}{2}} = \frac{V_{\text{circ}}^2}{R}$$

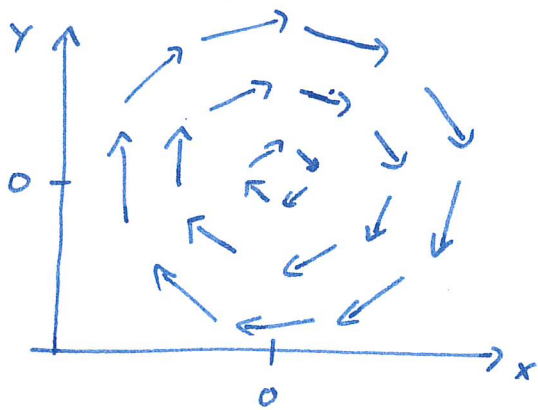
$$\Rightarrow V_{\text{circ}} = \frac{R}{h} \left[ 1 + \frac{R^2}{h^2} \right]^{\frac{\rho-2}{4}}$$

Results:

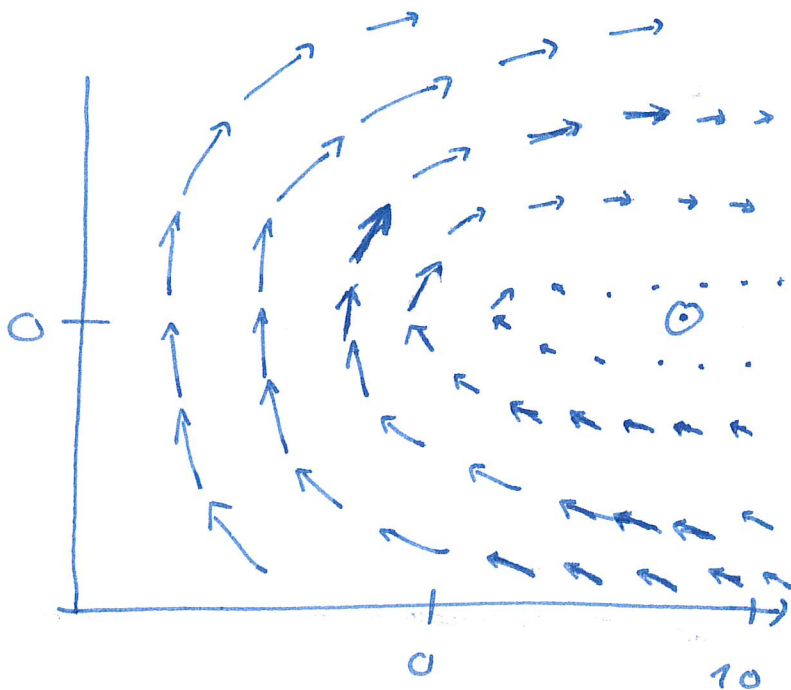


See printed plots for more details.

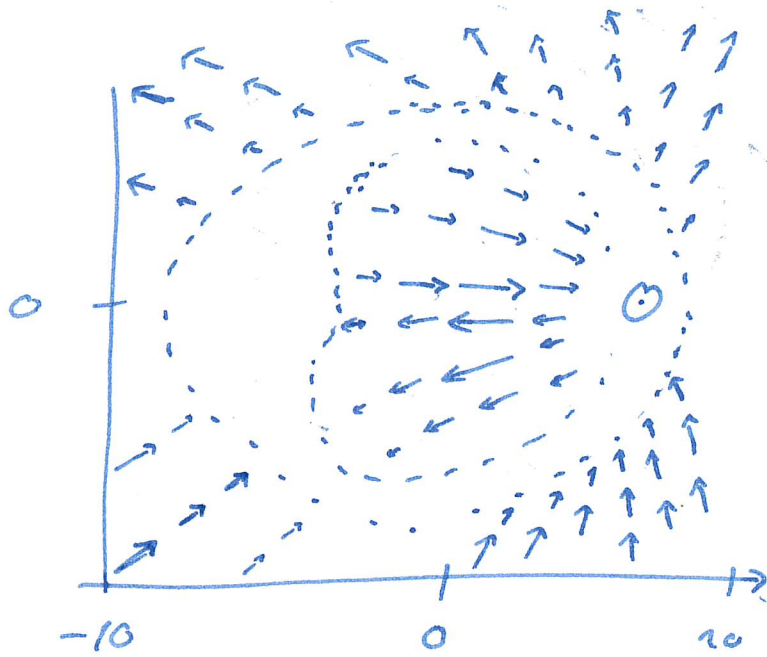
The circular velocity field of such a potential looks nicely symmetrical:



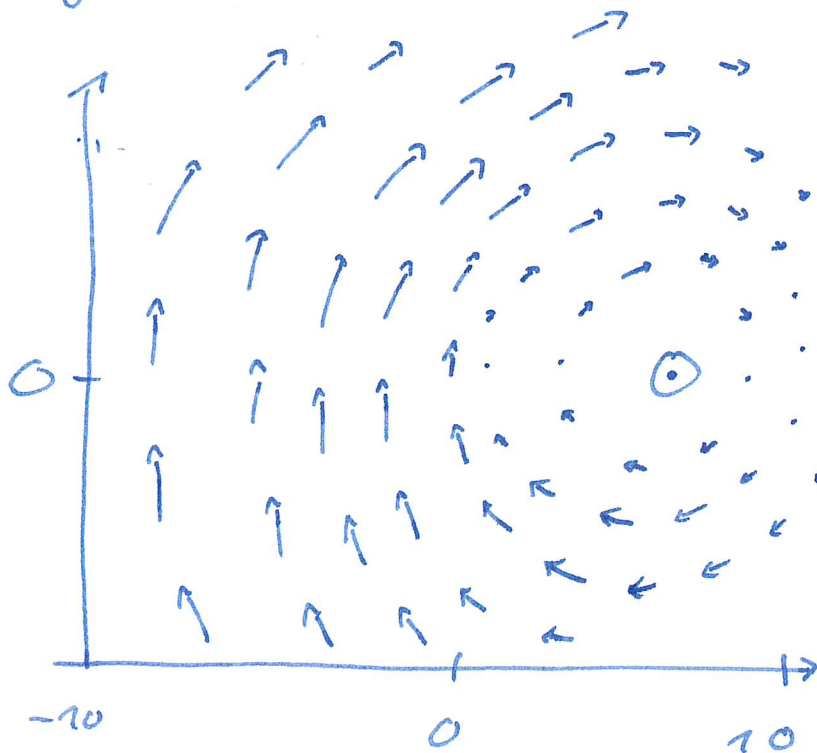
In the reference frame (LSR) of the sun (assuming  $x_{\odot} = 8 \text{ kpc}$ ,  $y_{\odot} = 0$ )



The radial velocity field looks like:  
(w.r.t. the sun's LSR)

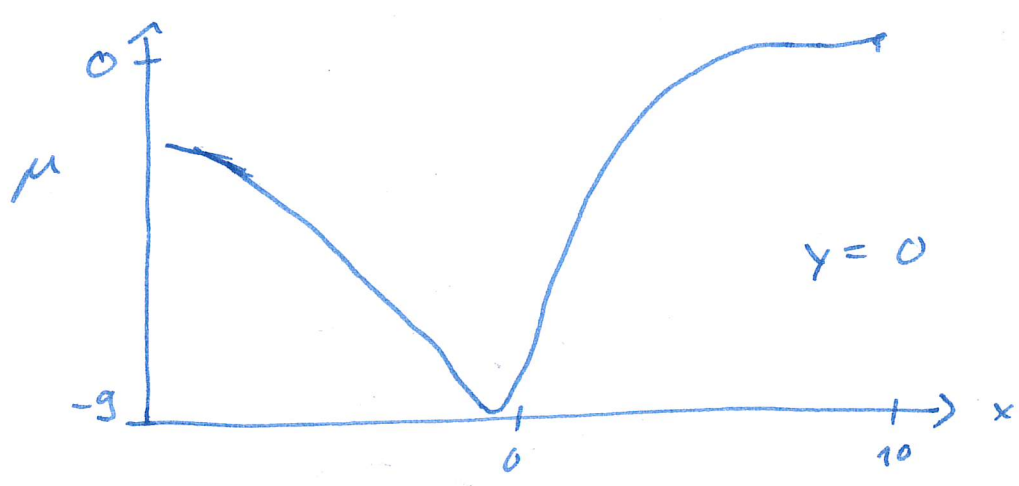
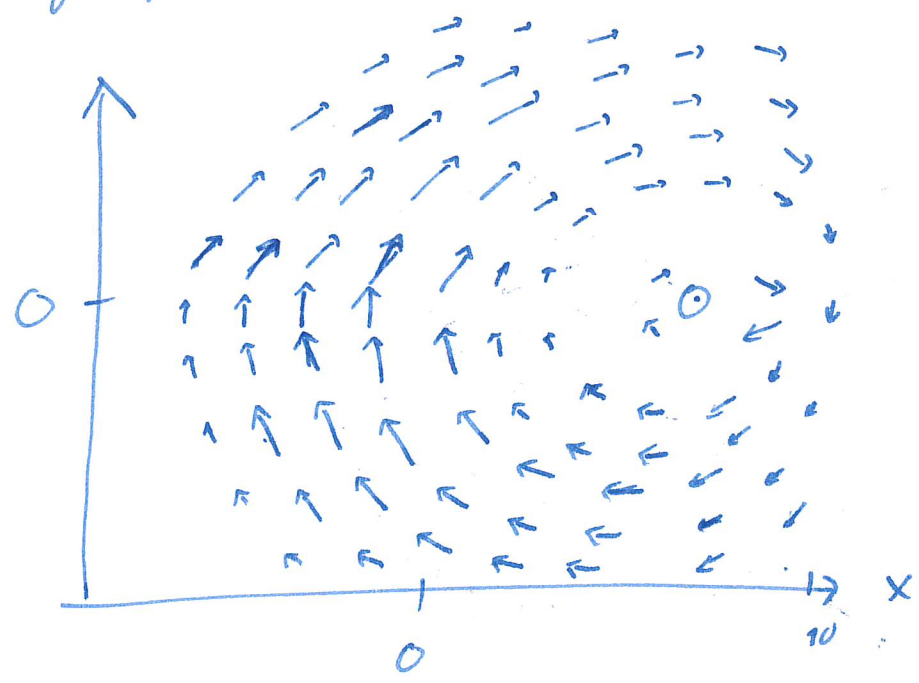


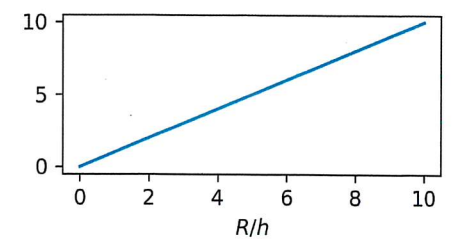
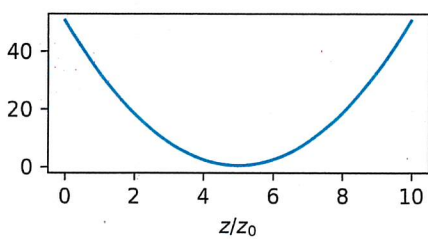
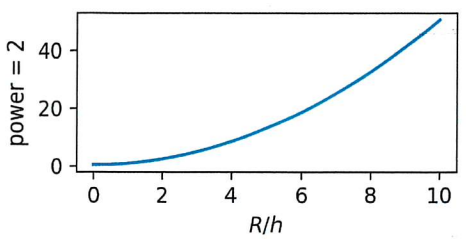
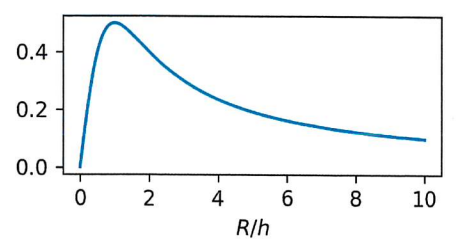
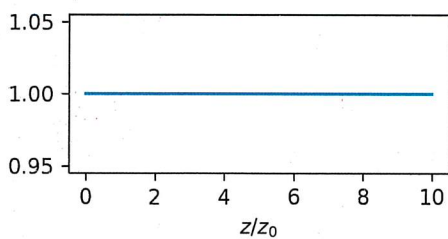
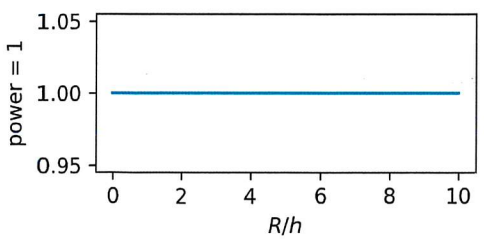
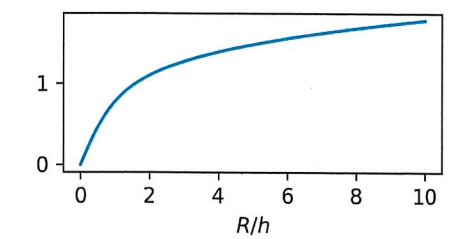
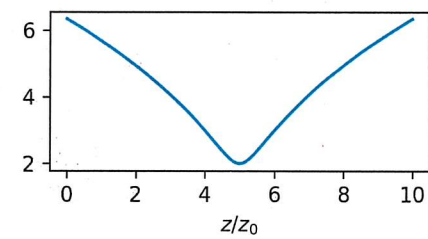
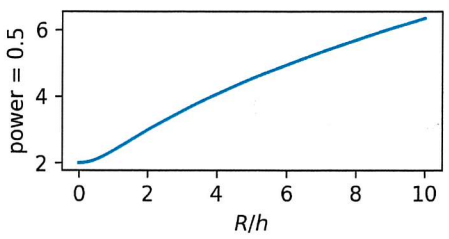
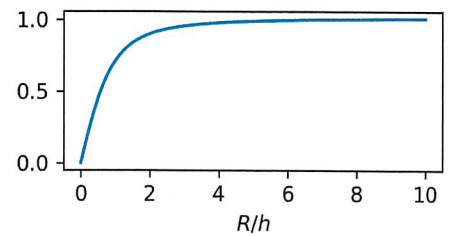
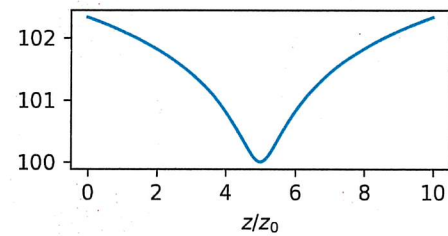
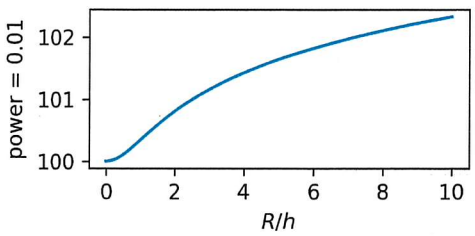
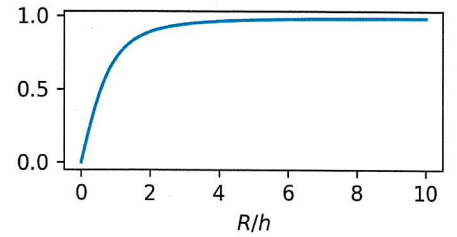
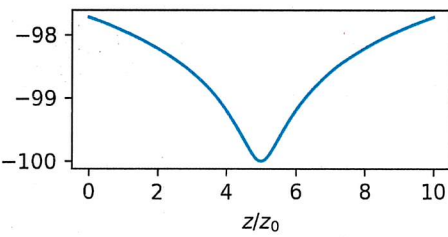
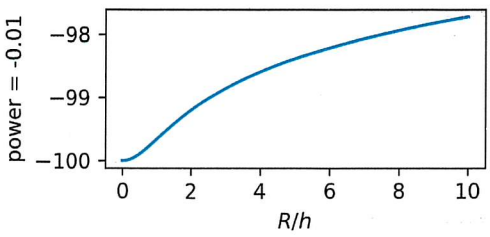
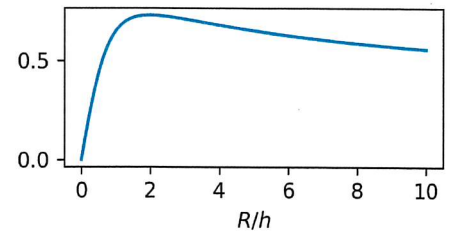
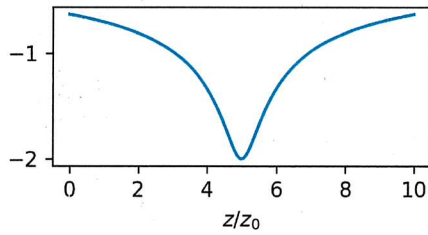
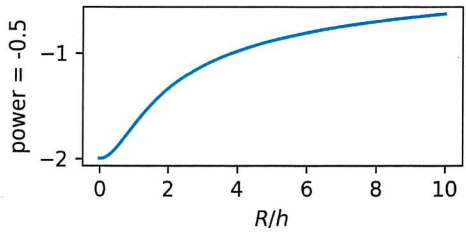
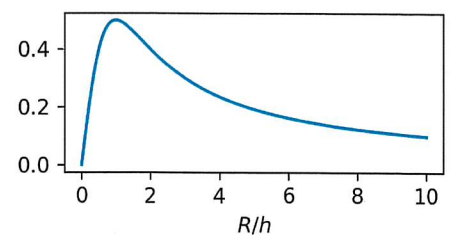
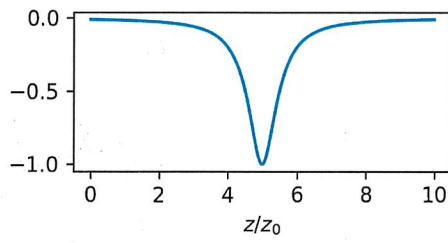
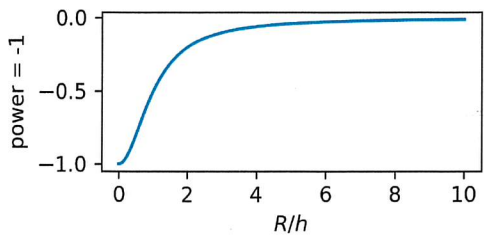
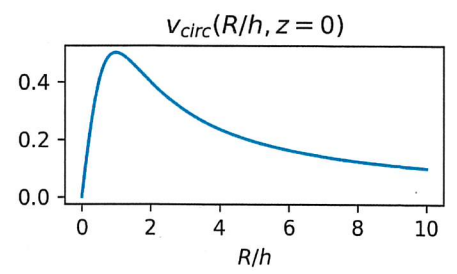
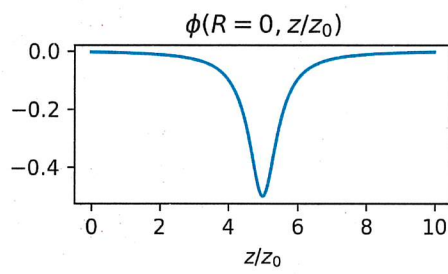
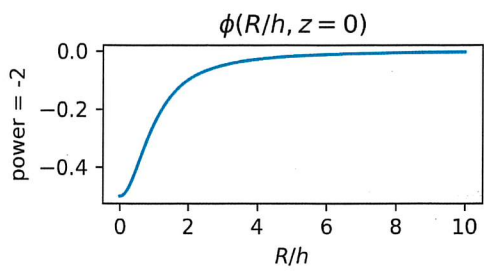
The tangential velocity field looks like:

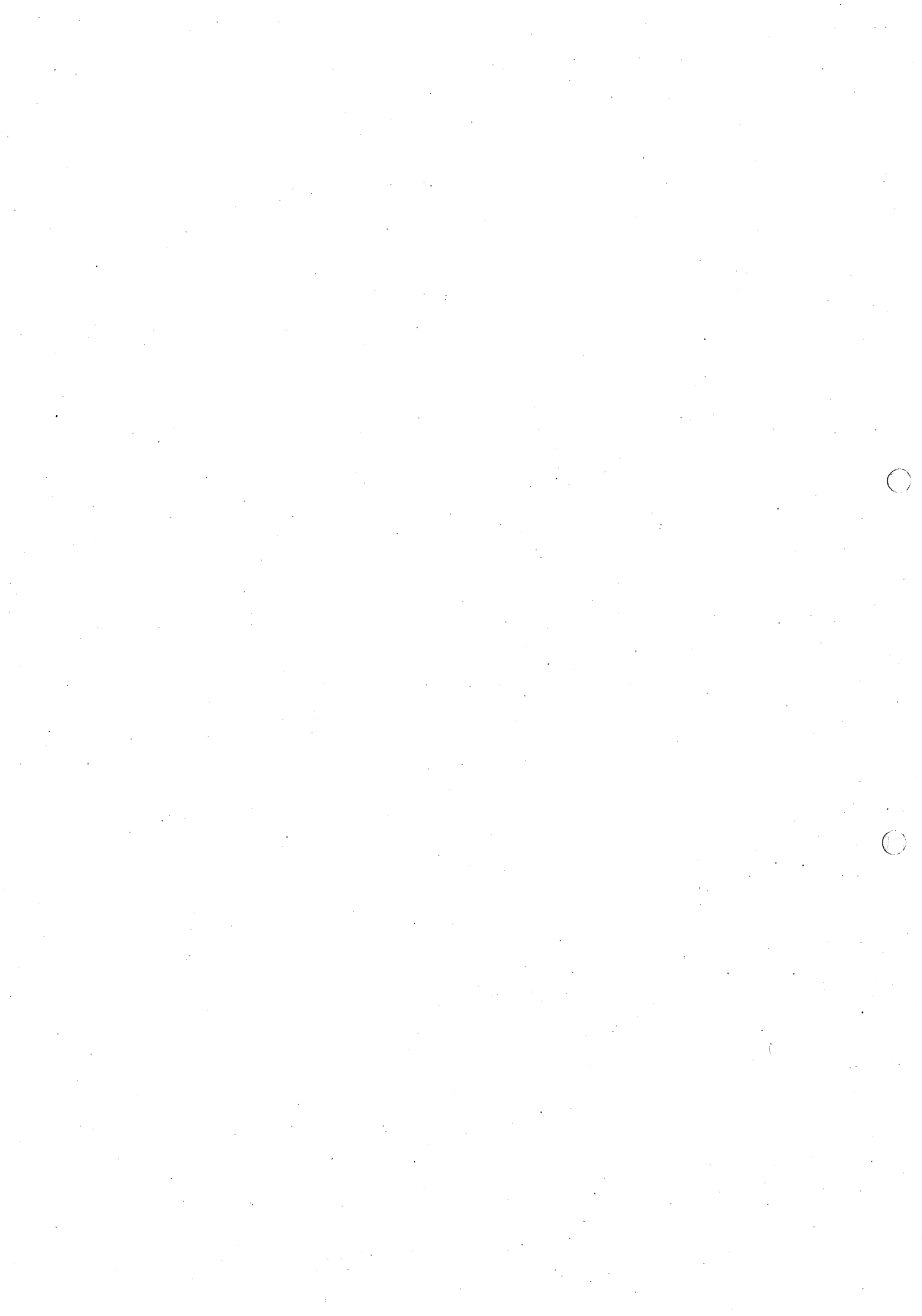




The proper motion  $\vec{\mu} = \frac{\vec{V}_t}{d}$  looks like:









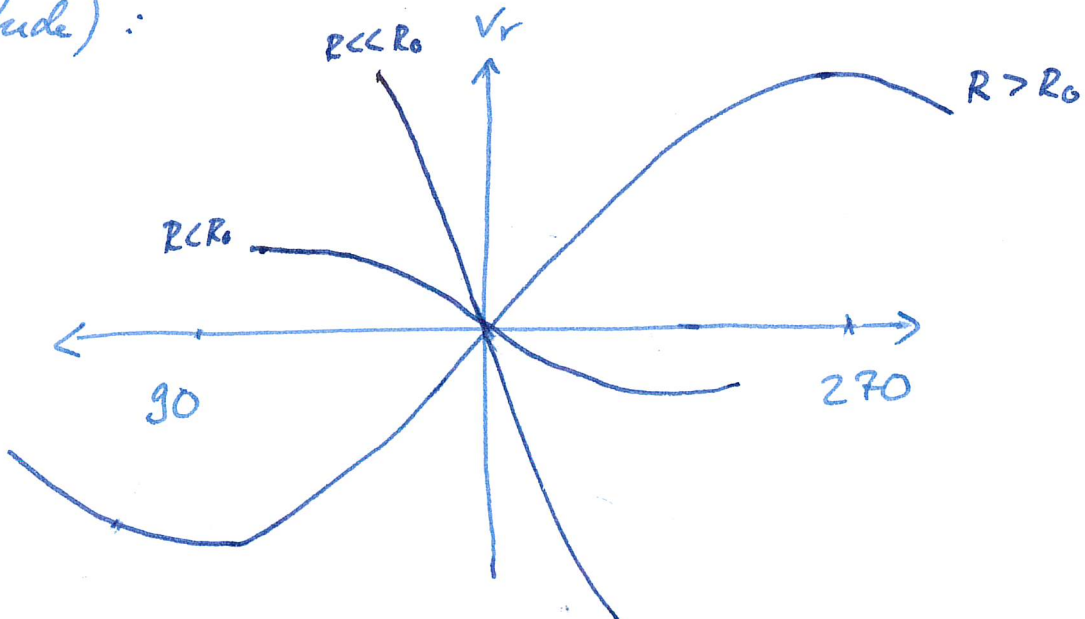
## MISC NOTES / ADDENDA

Note that for dynamical reasons, a purely circulating rotating self-gravitating is violently unstable. A minimal radial velocity is required for stability.

We saw that

$$v_r = (\Omega - \Omega_0) R_0 \sin l$$

which of course means that if you observe different positions of the MW, you should get different radial velocities based on the position (longitude):



this plot assumes circular orbits in an axis-symmetric disk, and that the observed stars are in the galactic plane.

Normally,  $\Omega$  is a decreasing function of  $R$ .

Crude estimate:

$$\Omega = \frac{v_{\text{rot}}}{R}; \quad \frac{v_{\text{rot}}^2}{R} = \frac{GM(R)}{R^2} \Rightarrow \Omega = \sqrt{\frac{GM(R)}{R^3}}$$

For a uniform disk, we have  $M(R) = \int_0^R 2\pi h r dr \rho_0$   
 $\propto R^2$

$\Rightarrow \Omega(R) \propto \frac{1}{\sqrt{R}}$  decreases with  $R$

$\Rightarrow \Omega - \Omega_0 < 0$  for  $R > R_0$

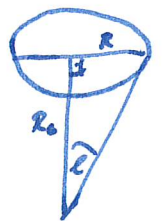
$\Omega - \Omega_0 > 0$  for  $R < R_0$

$\Rightarrow$  we get negative sine curve for  $R > R_0$   
[note that the angle  $\ell$  increases towards the left direction in the plot on the previous page]

Furthermore, we note:

• For  $R < R_0$ :

the curve is not a full sine, but a section between  $\pm \ell_{\text{max}}$  with  $\ell_{\text{max}} = \arctan \frac{R}{R_0}$



• For  $R > R_0$ : (ring outside solar circle)

The ring traces a full sine curve, albeit a negative one.

• Because  $\Omega(R) \propto 1/\sqrt{R}$ :

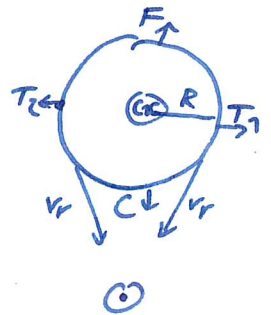
$$\bullet \left. \frac{\partial v_r}{\partial l} \right|_{l=0} = (\Omega - \Omega_0) R_0 \cos l \Big|_{l=0} \propto (\Omega - \Omega_0)$$

around  $l=0$ , the slope of the curve at  $l=0$  is proportional to  $\Omega - \Omega_0$

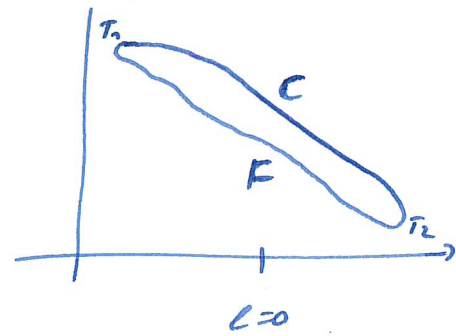
• This slope/difference is largest for largest  $\Omega(R) \rightarrow$  as close to the center as possible

How does this curve behave if the rings aren't static, but expand or contract radially while rotating?

The tangent points  $T_1$  &  $T_2$  are unchanged. The point close to us, C, will have increased radial velocity, while the one far from us, F, will have negative radial (line-of-sight) velocities.



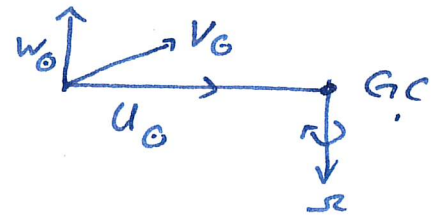
$\Rightarrow$  The expansion causes the section of a sine curve predicted by circular rotation opens up into a curved loop.





# Average Velocities according to colour subsamples

Usually the sun's velocity components are defined as follows:

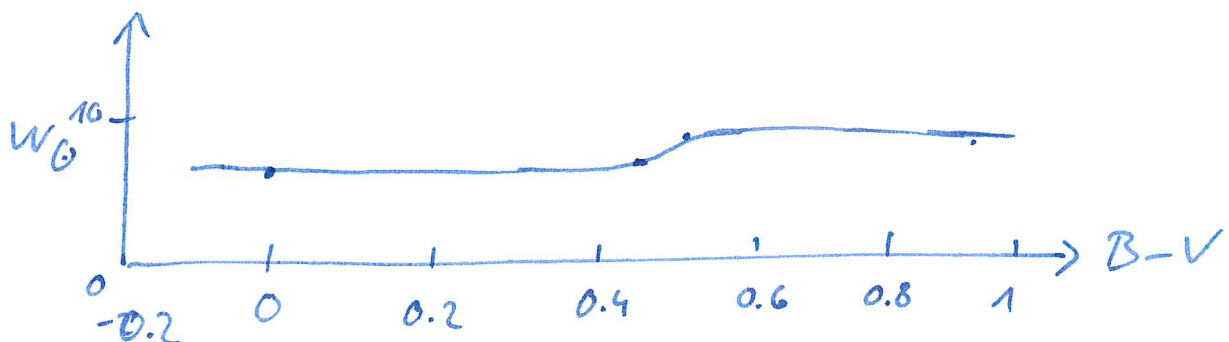
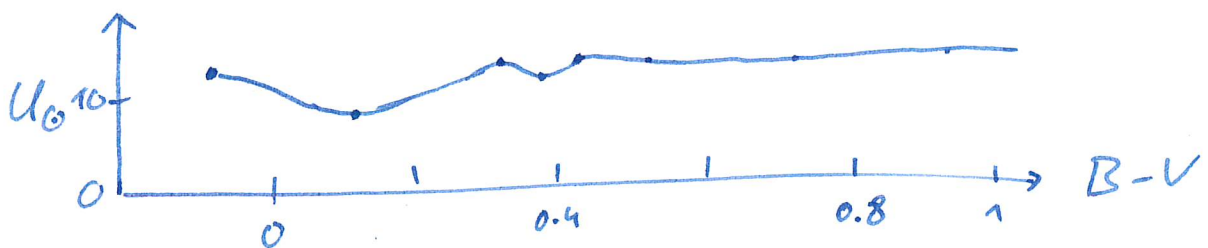
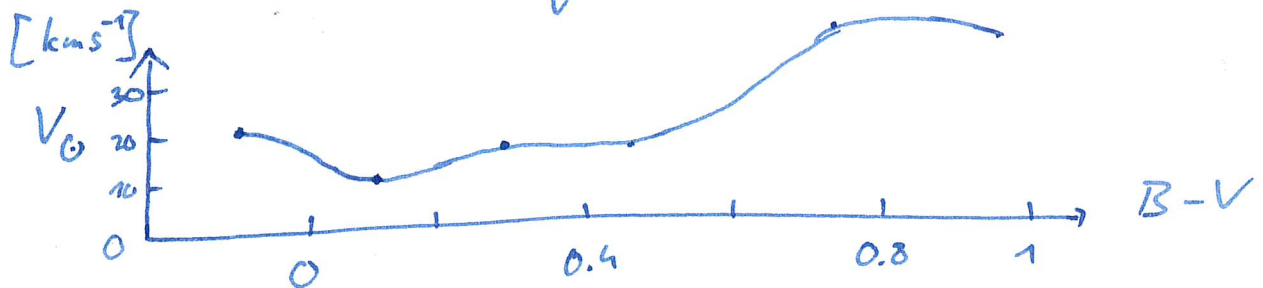


$U_{\odot}$ : towards galactic center

$V_{\odot}$ : tangential velocity along direction of disk rotation

$W_{\odot}$ : component perpendicular to the disk.

The average velocities of the sun have been measured and computed for different colours:



The sun rotates in the disk faster ( $\sim 10 \text{ km/s}$ ) with respect to the red star sample ( $B-V > 0.6$ ) than w.r.t. the blue star sample ( $B-V < 0.4$ )

In summary, the Sun's motion w.r.t. the LSR is

$$\left. \begin{array}{l} U_{\odot} \sim 10 \text{ km/s} \\ V_{\odot} \sim 5 \text{ km/s} \\ W_{\odot} \sim 7.2 \text{ km/s} \end{array} \right\} |V_{\odot}| = 13.4 \text{ km/s}$$

[Note: In 2011 paper, based on metallicity gradient they correct  $V_{\odot} \sim 12 \text{ km/s}$ ]

The Sun is moving toward the Galactic Center, up toward the north Galactic pole and is moving around the Galactic center faster than it would on a circular orbit.

We should give  $V_0$  some special attention.

For  $B-V < 0.61$ ,  $V_0$  increases steadily, while for  $B-V > 0.61$ ,  $V_0$  is independent of  $B-V$ .

This steady increase is a reflection of a phenomenon called asymmetric drift, which is the tendency of the mean rotation velocity of a stellar population to lag behind that of the LSR more and more with increasing random motion within the population.

It is fair to assume that the older red stars have a higher velocity dispersion, thus higher random motion, which leads to a higher asymmetric drift. When the Sun's velocity is referred to such a lagging reference frame, it acquires a value of  $V$  which grows as the lag increases.

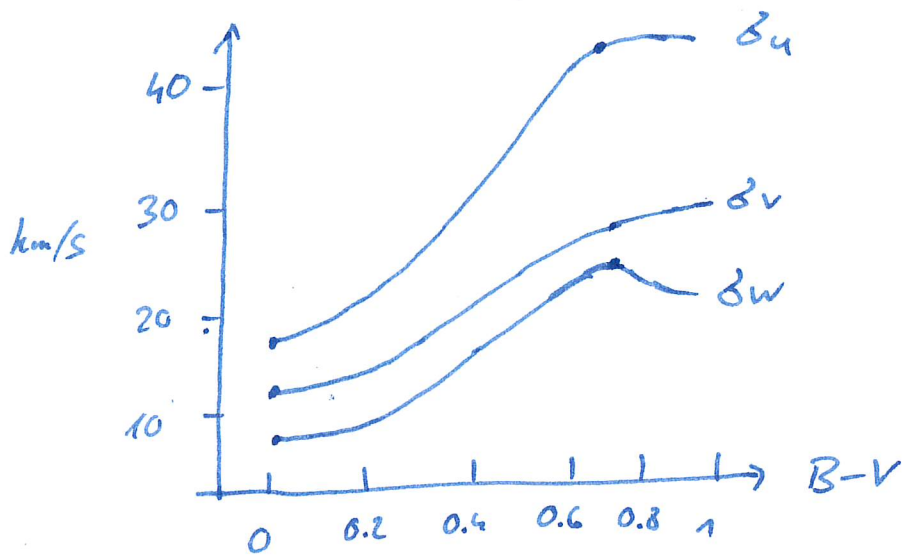




# Velocity Dispersion of the Local Stars

For every velocity component  $k$ , the velocity dispersion is defined as the standard deviation:

$$\sigma_k \equiv \langle (u_k - \langle u_k \rangle)^2 \rangle^{1/2} = \sqrt{\frac{1}{N} \sum_i (u_{k,i} - \frac{1}{N} \sum_{j=1}^N u_{k,j})^2}$$



We notice two important things:

- we always have  $\delta_u > \delta_v > \delta_w$

( $\delta_R > \delta_T > \delta_B$ )

for any colour! The ratios are  $\frac{\delta_v}{\delta_u} \sim 0.6$ ,  $\frac{\delta_w}{\delta_u} \sim 0.5$

- blue stars ( $B-V < 0.4$ ) have smaller dispersions and therefore smaller random motions than red stars ( $B-V > 0.6$ )

Computing the velocity dispersions for different spectral types of stars (OBAFGKM), which starts with giant, hot stars (OB) and ends with small, cold stars (KM), shows that the velocity dispersions in any direction tends to increase with decreasing size and temperature of the stars.

Smaller stars tend to be older, since giant stars evolve much faster throughout their life.

So in general, the velocity dispersions tend to increase with the stellar age.

The fact that  $\sigma_u \neq \sigma_v$  [ $\sigma_R \neq \sigma_T$ ] indicates that the distribution function of the stars for a simple galaxy model isn't right and invalidates some of the assumptions that:

- the distribution function is axisymmetric
- the distribution function is not static, i.e. depends on time
- the distribution doesn't depend on conservation along the  $z$ -axis

Old stars keep the information about the Milky Way at their formation time and are perturbed.

Stars bluer than  $B-V \approx 0.6$  are all younger than  $\sim 10$  Gyr. Redder stars are a mixture of a few young stars and mostly old stars. The fact that they have systematically larger velocity dispersions suggests the operation of a mechanism that leads to a progressive increase of the dispersion over time, like disk instabilities, influence of the spiral arms, merging events, etc.





## Vertex Deviation and Velocity Ellipsoid

The velocity dispersions in any direction  $k$  can be computed as

$$\sigma_k = \sqrt{\langle (v_k - \langle v_k \rangle)^2 \rangle}$$

In addition, one can average products of velocity components  $(v_i - \langle v_i \rangle)(v_j - \langle v_j \rangle)$ ,  $i \neq j$  instead of  $(v_k - \langle v_k \rangle)^2$ . can be left out for  $v_k: \langle v_k \rangle \approx 0$

For all stellar types, the averages of such products that involve  $v_z$  are smaller than the errors, but the average  $\langle v_x (v_y - \langle v_y \rangle) \rangle$  is significantly different from zero. For stars of those types,  $v_x$  and  $v_y$  are not statistically independent: If  $\langle v_x (v_y - \langle v_y \rangle) \rangle > 0$ , then for a positive measured  $(v_y - \langle v_y \rangle)$ , that star is more likely to have a positive  $v_x$ .

In this case, it helps to find linear combinations of the observables which are statistically independent.

We define:

$$v_1 \equiv v_x \cos \theta_v - (v_y - \langle v_y \rangle) \sin \theta_v$$

$$v_2 \equiv v_x \sin \theta_v + (v_y - \langle v_y \rangle) \cos \theta_v$$

Note that we have this formulation for  $\langle v_x \rangle \neq 0$ , otherwise  $v_x$  would be replaced by  $(v_x - \langle v_x \rangle)$ .

We want  $v_1$  and  $v_2$  to be statistically independent, therefore we set

$$\langle v_1 v_2 \rangle \stackrel{!}{=} 0$$

$$= \left\langle \left( \underbrace{v_x^2}_{\text{with } \langle v_x \rangle \neq 0: \sigma_x^2 = \langle v_x^2 \rangle - \langle v_x \rangle^2 \approx \langle v_x^2 \rangle} - (v_y - \langle v_y \rangle)^2 \right) \sin \theta_v \cos \theta_v - v_x (v_y - \langle v_y \rangle) (\cos^2 \theta_v - \sin^2 \theta_v) \right\rangle$$

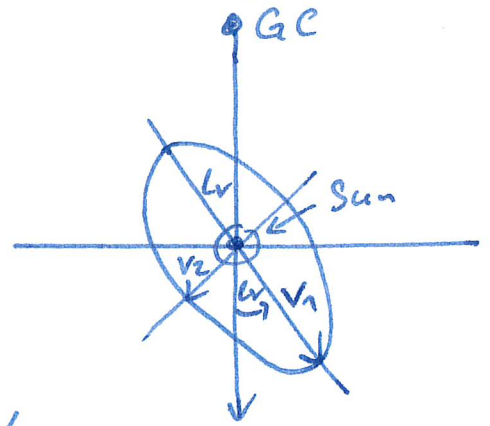
$$\approx \frac{1}{2} (\sigma_x^2 - \sigma_y^2) \sin 2\theta_v - \langle v_x (v_y - \langle v_y \rangle) \rangle \cos 2\theta_v$$

$$\Rightarrow \tan 2\theta_v = \frac{\frac{1}{2} (\sigma_x^2 - \sigma_y^2)}{\langle v_x (v_y - \langle v_y \rangle) \rangle}$$

$$\Rightarrow \theta_v = \frac{1}{2} \arctan \left( \frac{\frac{1}{2} (\sigma_x^2 - \sigma_y^2)}{\langle v_x (v_y - \langle v_y \rangle) \rangle} \right)$$

this is the condition for  $v_1$  and  $v_2$  to be statistically independent. To avoid ambiguity, we chose  $\sigma_1 \equiv \langle v_1^2 \rangle^{1/2} > \sigma_2 \equiv \langle v_2^2 \rangle^{1/2}$

This linear transformation from  $v_x$  and  $v_y - \langle v_y \rangle$  is a rotation of coordinates, so  $v_1, v_2$  are simply components of velocity in directions that are inclined by  $\iota_r$  to the center-anticenter direction.



If we draw the ellipse marked with semi-axes  $\sigma_1$  and  $\sigma_2$ , then the mean square of any component of velocity in any direction will be on the ellipsoid. (Same in 3D with additional  $\sigma_z$ .)

This surface is called the velocity ellipsoid. For all types of stars in the solar neighbourhood, one of its principal planes coincides with the plane of the Milky Way, but its longest axis deviates from the center-anticenter direction by the vertex deviation  $\iota_r$ .



The vertex deviation decreases with increasing B-V from  $\sim 30^\circ$  for the bluest (youngest) stars to  $\sim 10^\circ$  for the reddest (oldest stars).

This behaviour is opposite to the velocity dispersion, which increases with red/age!

What are the causes of vertex deviation?

- Moving groups of stars: If a significant fraction of the measured stars are members of a few distinct moving groups, leading to error underestimation and statistical noise.
- Non-axisymmetric component of the Galactic potential. (Bar, Spirals...)
- Time-dependence of the interaction between bar and spirals: The bar is not completely rigid, and is rotating at a  $\sim 2-3$  higher angular velocity than the spirals, leading to reciprocal perturbations between the bar and spirals.



# Complete Velocity Distribution

Plotting the number densities of stars on the  $U-V$  plane for different  $B-V$  ranges reveals the following:

(Fig. 10.15 Binney/Merrifield)

- The distribution spreads with increasing  $B-V$  (with "increased red"). The increase of all  $\sigma_i$  with  $B-V$  quantifies this phenomenon.
- The maps show a clear tendency for the region of highest stellar density to be elongated along a line that slopes from bottom left to top right. The vertex deviation quantifies this effect.

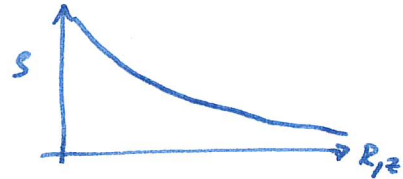
- There are tight clumps present.  
These correspond to star streams, which are groups of stars moving along the same speed in the same direction. They are thought to be vestiges/remnants of clusters and associations in which most of the stars form, even though currently they may not be spatially close to each other (any more). [Conclusive proof comes from plotting color-magnitude diagrams of these stars and getting typical shapes]

# Galactic Disk

## Stellar Disk

The stellar disk is well described by a double exponential law:

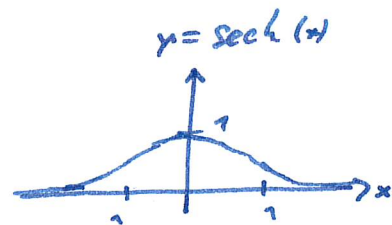
$$\rho(R, z) = \rho_0 e^{-R/h} e^{-|z|/h_z}$$



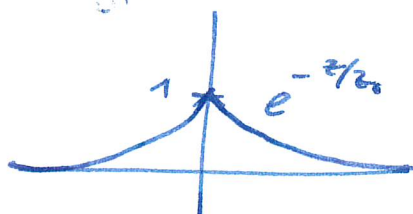
unless you're looking at the center when  $z=0$ .  
There, the density is better described by a sech function

$$\rho = \rho_0 e^{-R/h} \operatorname{sech}^2\left(\frac{z}{2h_z}\right)$$

where  $\operatorname{sech} = \frac{1}{\cosh} = \frac{1}{\frac{e^x + e^{-x}}{2}}$



because the exponential gives a sharp peak  
otherwise:

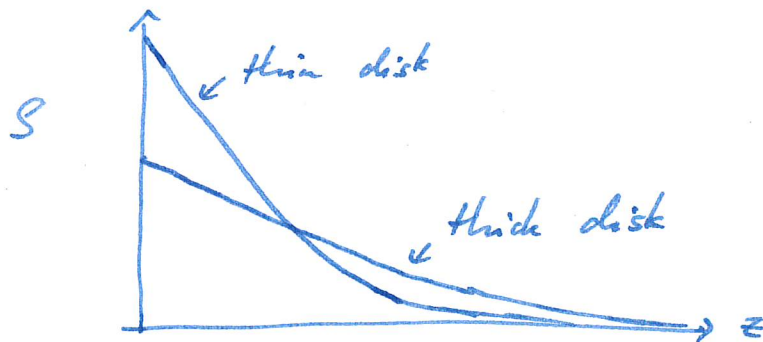


We differentiate between the thin and thick stellar disk:

$h \sim 3 \text{ kpc}$  scale length for  $R$

$h_{z, \text{thin}} \sim 300 \text{ pc}$  scale length for  $z$  for thin disk

$h_{z, \text{thick}} \sim 900 \text{ pc}$  scale length for  $z$  for thick disk



This density is actually observed, but not reason enough to justify 2 disks. The difference in ages and metallicities however is.

The disk mass can be computed as

$$\begin{aligned}
 M_{\text{Disk}} &= \int dV S = 2\pi \int R dR \int dz S(R, z) = \\
 &= 2\pi \int_0^{\infty} R dR \int_{-\infty}^{\infty} dz S_0 e^{-R/h} e^{-|z|/h_z} \\
 &= 2\pi S_0 \int_0^{\infty} R dR \cdot 2 \int_0^{\infty} e^{-R/h} e^{-z/h_z} dz \\
 &= 2\pi S_0 \int_0^{\infty} R dR e^{-R/h} \cdot 2 \int_0^{\infty} e^{-s} \cdot h_z ds \\
 &= 4\pi S_0 \int_0^{\infty} R dR e^{-R/h} \left[ -e^{-s} \right]_0^{\infty} h_z = \\
 &= 4\pi S_0 \int_0^{\infty} R dR e^{-R/h} h_z = 4\pi S_0 \left[ -h e^{-R/h} (h+R) \right]_0^{\infty} h_z \\
 &= \underline{4\pi S_0 h_z h^2}
 \end{aligned}$$



The luminosity of the stellar disk also follows an exponential law:

$$L(R) = L_0 \exp(-R/h_r)$$

and is thus proportional to the density of the disk.

The thin stellar disk:

- has 85% of the stars in the galactic plane and 95% of the total disk stars

- is more metal rich

- is younger than the thick disk

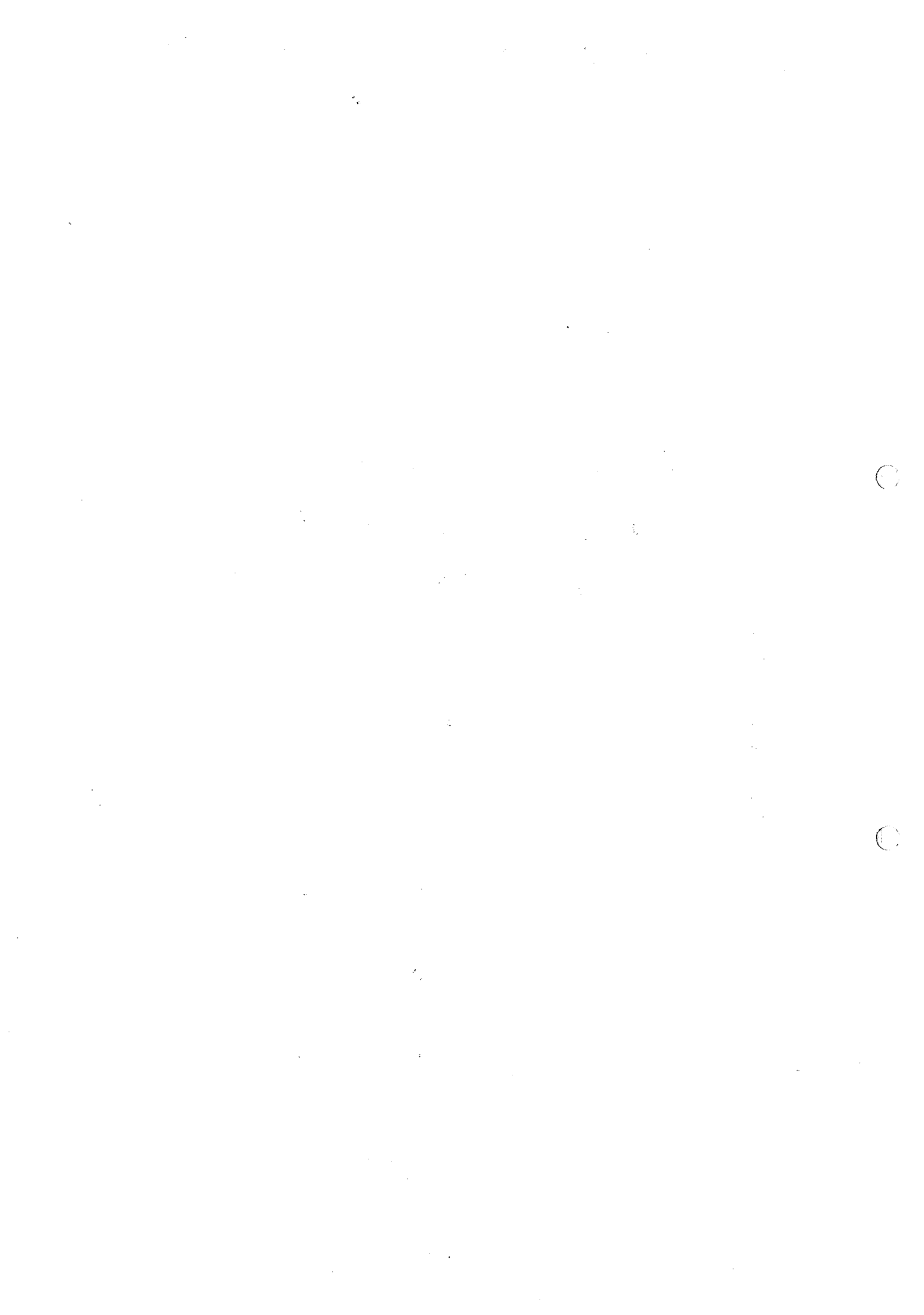
- has mass  $\sim 12 \cdot 10^3 M_\odot$

The thick stellar disk:

- is almost exclusively composed of old stars

- has a low metallicity

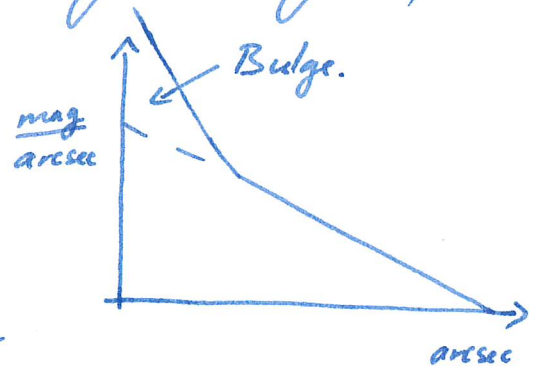
- has mass  $\sim 50 \cdot 10^3 M_\odot$



# Bulge

The bulge is at the center of the galaxy.

It has a density function steeper than an exponential and is identifiable (in other galaxies) as excess light, steeper than the exponential, around the center. Note that the plot above is in a logarithmic scale, since magnitudes are plotted.



The bulge resembles a bit a (small) elliptical galaxy and follows De Vaucouleur's luminosity law:

$$\log \left( \frac{I(r)}{I_0} \right) \propto - \left[ \left( \frac{r}{R_0} \right)^{1/4} - 1 \right]$$

where  $I_0 = I(R_0)$ .

General practice: Bulge  $\approx \pm 10^\circ$  in both longitude and latitude (no sharp edges can be defined.)

Data suggest that it is a Box/Peanut shaped bulge, which is common in spiral galaxies. It also has a common X-shaped component in the bulge.



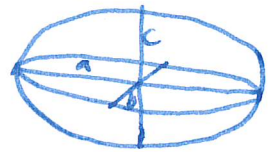
face-on contour lines



edge-on contour lines

More generally, its shape is a oblate spheroid:

$$m^2 = \frac{x^2}{a^2} + \frac{y^2}{b^2} + \frac{z^2}{c^2}$$



For an oblate spheroid, we have

$$a = b > c$$

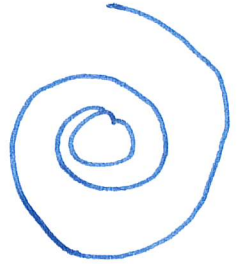
For the Bulge:  $a = b = 3 \text{ kpc}$ ,  $c = 1.5 \text{ kpc}$



## Spiral Arms

The central idea of the theory of spiral structure is that spiral arms will form if stars and gas clouds move on elliptical orbits whose major-axis positions vary smoothly with increasing radius.

Plotting a lot of such orbits starting at different directions from the center and assuming that every orbit/oval is uniformly populated with gas clouds and stars.

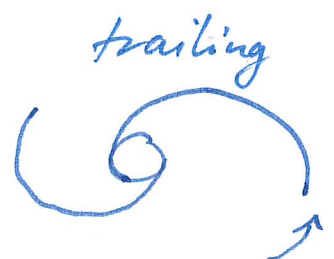
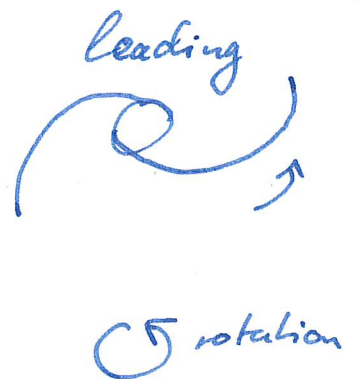


Provided that the directions of the long axes rotate enough over the disk (in image 9.9 in Binney/Merfield:  $>540^\circ$ ) in some regions, the ovals are much closer to each other than in others. If every oval is uniformly populated, this results in spiral-like surface densities.

Grand-design spirals are spirals that are long, continuous and symmetric arms. Presumably, they have been formed by some large scale global process that involves the whole galaxy.

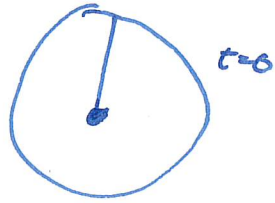
Grand-design spiral galaxies almost always have two main arms. Often in the images the spirals are accompanied by thin dark stripes, caused by absorption of the galaxy's starlight in dense clouds of gas and dust, called dust lanes. These generally follow the spiral arms.

Spiral arms can be classified by their orientation relative to the direction of rotation of the galaxy, more precisely the orientation of the tip of the spiral arm.



The pitch angle of an arm is defined at any radius  $R$  as the angle  $\alpha$  enclosed between the tangent to the arm and the circle  $R = \text{const.}$

If we would set a narrow stripe radially across the galactic disk at some initial time  $t=0$  and assume a flat rotation curve, of the disk, then the disk will have differential rotation, meaning  $\Omega(R) \neq \text{const.}$



Now letting such a galaxy rotate for a few Gyrs undisturbed, the pitch angle at around the Sun's position in the disk of the arm will be  $\ll 1$ , which is much smaller than observed. This discrepancy is called the winding problem.

It is more likely that spirals are stationary density waves in the stellar density (Lin-Shu theory.)



Spirals contain many young stars  $\approx 10$  Myr of age, which is much less than a typical rotation time of  $\approx 100$  Myrs. Also H II regions are strung out like pearls along the arms, leading to the conclusion that the star-formation rate in spiral arms is much higher than in the rest of the disk. The young stars are traced in blue light.

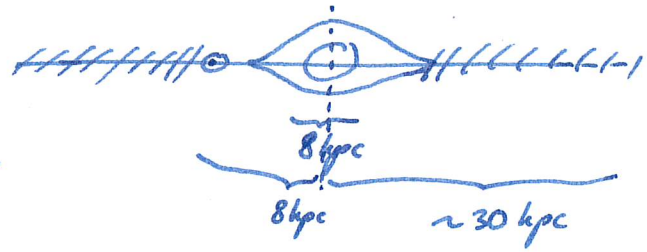
Near-infrared traces mass, since its absorption is much less severe through dust and its source is mostly giant stars, which are older. In NIR, the arms are smoother and broader, probably because the irregular spatial distribution of star formation sites has been phase-mixed away in the old stars.

The presence of spiral structure in the old stars that dominate the mass is common to most grand-design spiral galaxies, and implies that the entire stellar disk participates in the spiral pattern.



# Gaseous Disk

The Milky Way has a gaseous disk which reaches out to  $\sim 3 R_{\odot} \sim 24-30 \text{ kpc}$ .




We can trace  $\text{H}_2$  through the  $\text{CO}(2-1)$  rotation line and  $\text{HI}$  by its  $21 \text{ cm}$  line emission.

The presence of  $\text{H}_2$  also reveals the presence of dust, because dust is one of the most efficient "catalysts" to create  $\text{H}_2$  in low density regions. For  $\text{H}_2$  to be created from atomic hydrogen, a third body is needed, and large dust grains have higher interaction cross-sections.

The gaseous disk has a warp that becomes strong beyond the solar radius.

Possible causes for this warp are disk instabilities or satellite accretion of a satellite that had different angular momentum than the Milky Way.



The rotation curve of the disk is approximately flat, with

$$S_{\text{total}} \sim 1/r^2$$

$$M(r) \propto r$$

# Energy of a Galaxy

To estimate the energy budget of a galaxy, first we need to have a look at the virial theorem.

## The Virial Theorem

We start by writing down the moment of inertia for a system of  $N$  particles with masses  $m_i$ , positions  $\vec{x}_i$  and velocities  $\frac{d\vec{x}_i}{dt} = \vec{v}_i$ .

For such a particle system, the moment of inertia is defined as

$$I = \sum_{i=1}^N m_i \vec{x}_i \cdot \vec{x}_i$$

the moment of inertia, here with respect to the origin of the coordinate system, is a measure of the mass distribution.

Because it contains the sum over all  $|\vec{x}|^2$ , it is straightforward to see that

- if  $\frac{dI}{dt} > 0$  and masses constant, then the system on average increases in  $|\vec{x}|$ , thus the system is expanding
- using the same argument:  $\frac{dI}{dt} < 0 \Rightarrow$  system contracting
- $\frac{dI}{dt} = 0$ : system on average in equilibrium.

Deriving the moment of inertia w.r.t. time twice gives:

$$\frac{dI}{dt} = 2 \sum_i m_i \vec{x}_i \cdot \dot{\vec{x}}_i = 2 \sum_i m_i \vec{v}_i$$

$$\frac{1}{2} \frac{d^2 I}{dt^2} = \sum_i m_i \vec{v}_i^2 + \sum_i m_i \vec{a}_i$$

$$\text{with } \vec{a}_i \equiv \frac{d\vec{v}_i}{dt} = \frac{d^2 \vec{x}_i}{dt^2}$$

$$\begin{aligned} \Rightarrow \frac{1}{2N} \frac{d^2 I}{dt^2} &= \frac{1}{N} \sum_i m_i \vec{v}_i^2 + \frac{1}{N} \sum_i m_i \vec{a}_i \cdot \vec{x}_i \\ &= \langle m v^2 \rangle + \langle m \vec{a} \cdot \vec{x} \rangle \end{aligned}$$



We recognize:

$$\frac{1}{N} \sum_i m_i v_i^2 = \langle E_{kin} \rangle$$

assuming we only have gravity working, we have  $\vec{a}_i = -G \sum_{j \neq i} \frac{m_i m_j}{|\vec{x}_i - \vec{x}_j|^2}$

$$\text{and } \frac{1}{N} \sum_i m_i \vec{x}_i \cdot \vec{a}_i = \langle E_{grav} \rangle$$

giving us

$$\begin{aligned} \frac{1}{2N} \ddot{I} &= 2 \langle E_{kin} \rangle + \langle E_{grav} \rangle \\ &= 0 \text{ for systems in equilibrium} \end{aligned}$$

For fluids, we replace the discrete sum with a continuous integral for the moment of inertia:

$$I = \int_V \rho(\vec{x}) |\vec{x}|^2 dV$$

and arrive at a similar result:

$$\frac{1}{2} \ddot{I} = 2 \bar{E}_{kin} + \bar{E}_{grav} + 3 \bar{P} V - 3 \bar{P}_{ext} V + \dots$$

where  $\bar{P}$  is the average pressure and  $\bar{P}_{ext}$  the average external pressure at the boundary of the system.

# Energy Budget of the Galaxy

We can now estimate the energy budget of the galaxy:

o For the Milky Way: Kinetic Energy

$$E_{kin} = \frac{1}{2} M \langle v^2 \rangle = \frac{1}{2} M (v_{rot}^2 + \sigma^2)$$

$$M \sim 2 \cdot 10^{11} M_{\odot}, \quad v_{rot} \sim 200 \text{ km/s}, \quad \sigma \sim 30 \text{ km/s}$$

$$\Rightarrow E_{kin} \sim 10^{59} \text{ erg}$$

o ISM:

The energy density of the ISM is  $\sim 1 \text{ eV/cm}^3$ . For a disk with radius 15 kpc and height of 1 kpc, this gives a total energy of  $E_{ISM} \sim 10^{49} \text{ erg}$

$\Rightarrow$  not significant compared to  $E_{kin}$  of the Milky Way.

o Gravitational Energy:

Assuming a uniform sphere, we have

$$E_{grav} \sim -\frac{3}{5} \frac{GM^2}{R} \sim -1.6 \cdot 10^{59} \text{ ergs}$$

Clearly the kinetic and gravitational energies dominate.

- Radiation

$$L_{\text{rad}} \sim 2 \cdot 10^{44} L_{\odot} \sim 8 \cdot 10^{44} \text{ ergs/s}$$

on the short term, it's clearly not a dominant effect. However, over long periods of time, e.g. 10 billion years, we get

$$L_{\text{rad}} \cdot \tau = 8 \cdot 10^{44} \frac{\text{ergs}}{\text{s}} \cdot 10^9 \text{ yrs} \cdot 3 \cdot 10^7 \text{ s/yr} \sim 3 \cdot 10^{55} \text{ ergs}$$

so over long periods of time, the radiation can be a significant effect.

- Supernovae:

Have a similar contribution in the power as the radiation. A typical SN releases  $E_{\text{SN}} \sim 10^{51}$  erg in mechanical energy, at a frequency  $f \sim \frac{1}{30 \text{ yrs}}$ , giving

$$L_{\text{SN}} \sim 10^{42} \text{ ergs/s}$$

o Gravitational power:

We can estimate the maximal energy we can give to a system while it's changing its shape by

$$L_{\text{grav}} \sim \frac{-E_{\text{grav}}}{\tau_{\text{dyn}}} \sim \frac{-\frac{GM^2}{R}}{R/\langle v \rangle} \sim 4 \cdot 10^{43} \text{ erg/s}$$

Since radiation can deliver an order of magnitude more power, it is susceptible to change the galaxy slowly over time.



# Orbits of Stars in Galaxies

In general, the orbits of the stars are determined by the gravitational potential  $\phi(\vec{x})$ , which in turn is determined by the density distribution:

$$\nabla^2 \phi = -\nabla \cdot \vec{g} = 4\pi G \rho$$

Poisson's equation

$$\phi(\vec{x}) = -\int_V \frac{G \rho d^3x'}{|\vec{x} - \vec{x}'|^2}$$

Newton's law

It is useful to start off with idealised models, which we will do.

# Static Spherical Potentials

$$\phi = \phi(r)$$

$$4\pi G \rho(r) = \nabla^2 \phi = \frac{1}{r^2} \frac{\partial}{\partial r} (r^2 \partial_r \phi)$$

There are many used model potentials that include spherical symmetry:

- Point mass:  $\phi(r) = -\frac{Gm}{r}$

- Plummer:  $\phi(r) = \frac{-Gm}{\sqrt{r^2 + b^2}}$

- Isochrone model:  $\phi(r) = \frac{-Gm}{b + \sqrt{r^2 + b^2}}$

- Power law:  $\phi(r) = k \frac{r^p}{p} \quad -1 < p < 2$

- Harmonic oscillator:  $\phi(r) = \frac{1}{2} \omega^2 r^2$

Rotation curves in spherical symmetry (for circular orbits) are straightforward to obtain:

$$\frac{v_c^2}{r} = -a_r = \partial_r \phi(r) \Rightarrow v_c^2 = r \partial_r \phi(r)$$

Since the potential is assumed to be static, the energy  $E(\vec{x}, \dot{\vec{x}}) = \text{const.}$

$\Phi(r)$  is also independent of  $\varphi, \theta$ , meaning that angular momentum  $\vec{L}(r, \dot{r}) = \text{const.}$

(These can be derived with Euler-Lagrange equations and/or Hamiltonians)

Furthermore:  $\vec{L} = \vec{x} \times \vec{p} = \vec{x} \times m\vec{v} = m\vec{x} \times \dot{\vec{x}}$

$\Rightarrow \vec{L} \perp \vec{r}, \vec{L} \perp \dot{\vec{r}}, \vec{L} = \text{const}$

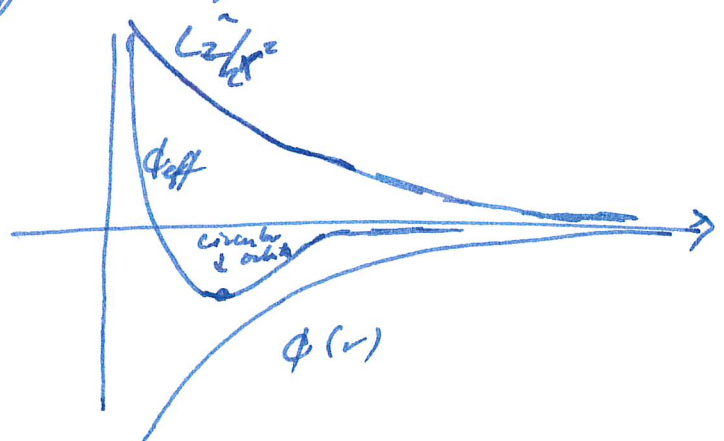
$\Rightarrow$  the motion is confined to a plane

The expression for the energy is

$$E = \frac{1}{2} (\dot{\vec{x}})^2 + \Phi(r) = \frac{1}{2} (\dot{r}^2 + \underbrace{(r\dot{\varphi})^2}_{L_2 = r^2\dot{\varphi} \text{ in sph. sym}}) + \Phi(r)$$

$$= \frac{1}{2} \dot{r}^2 + \frac{L_2^2}{2r^2} + \Phi(r)$$

Thus we can draw the effective potential, where we include the repulsive pseudo-potential of angular momentum



In general, the motion in a spherical potential will be confined between an inner radius (pericenter distance) and an outer radius (apocenter distance).

The radial period  $T_r$  is the time for the star to travel from apocenter to pericenter and back. While traveling from pericenter to apocenter and back, the azimuthal angle increases by an amount  $\Delta\phi$  in general. It can be shown that the azimuthal period

$$T_\phi = \frac{2\pi}{|\Delta\phi|} T_r, \text{ where } \frac{\Delta\phi}{2\pi}$$

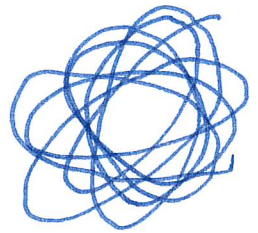


Fig. 3.1  
Binney/  
Tremaine

is in general not a rational number, thus the orbits won't be closed. There are exactly two potentials in which all orbits are closed, which are the harmonic oscillator

$$\phi(r) = \frac{1}{2} \omega^2 r^2$$

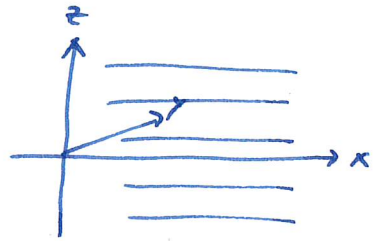
and the point mass potential

$$\phi(r) = \frac{GM}{r}$$



## Plane-Parallel geometry

Assume a geometry symmetric in  $x$  and  $y$ , neglecting the distance from the center



$$\Rightarrow \phi = \phi(z), \quad \partial_r \phi = 0, \quad \partial_\phi \phi = 0, \quad \partial_z \phi = -a_z$$

If we set  $\partial_z \phi(z=0) \stackrel{!}{=} 0$ , we may Taylor-expand:

$$\begin{aligned} \partial_z \phi &\cong \underbrace{\frac{\partial \phi}{\partial z}}_{=0} \Big|_{z=0} + z \underbrace{\frac{\partial^2 \phi}{\partial z^2}}_{\equiv v^2} \Big|_{z=0} + \mathcal{O}(z^4) \\ &\cong z v^2 \quad \left[ \frac{\partial^2 \phi}{\partial z^2} = 0 \text{ for symmetry} \right] \end{aligned}$$

$\Rightarrow$  To first order, the force is linear with  $z$

$\Rightarrow$  The potential is to first order a harmonic oscillator, giving closed orbits.

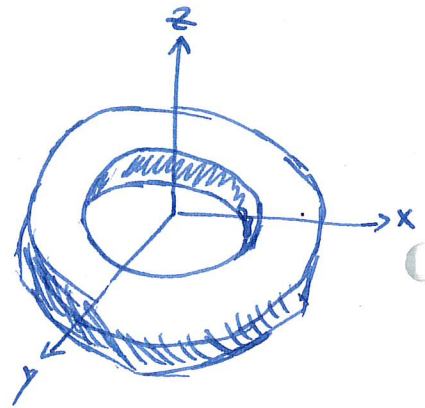
In galaxies however, this is not a good approximation. The non-linear terms are also important, giving the potential of an anharmonic oscillator, when the periods depend on the amplitude.

# Axisymmetric Stellar Systems

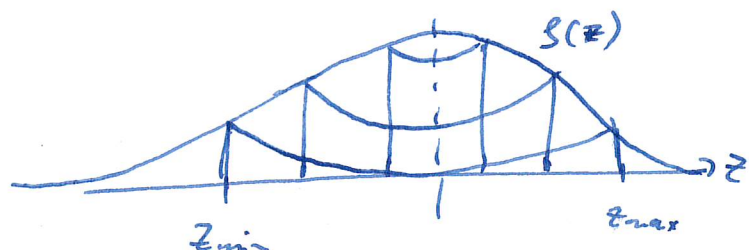
Assuming  $\phi(R, z) = \phi(R, -z)$

- Exactly on the  $z=0$  plane, we would get the same orbit as in spherical symmetry
- Close to the plane, we get the harmonic oscillator equation in the  $z$  direction. The stars oscillate between a  $z_{\min}$  and  $z_{\max}$ , but also move between a  $R_{\min}$  and  $R_{\max}$ :  $R_{\min}$  is set by the effective potential / angular momentum,  $R_{\max}$  by energy conservation.

A star, given enough time, will fill out a ring around the center



The total density can be reproduced as a superposition of orbits:



# Triaxial potentials, non-rotating

A triaxial potential is defined by

$$\Phi(x, y, z) = \Phi(\pm x, \pm y, \pm z)$$

which are ellipsoidal potentials, characterized by

$$m^2 = \frac{x^2}{a^2} + \frac{y^2}{b^2} + \frac{z^2}{c^2}$$

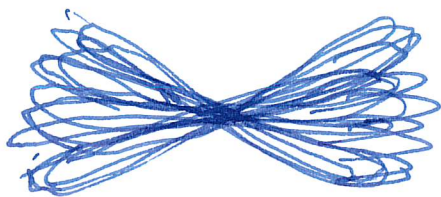
By convention,  $a \geq b \geq c$

The ellipsoid is called

- oblate:  $a = b$
- prolate:  $b = c$
- spherical:  $a = b = c$

Possible orbits in triaxial potentials are:

- Box orbits



The star eventually passes close to every point inside a rectangular box.

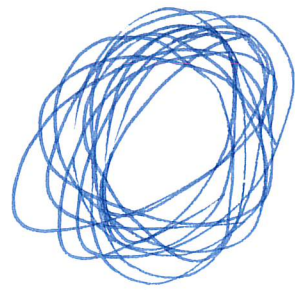
This is different from the ring orbits of a cylindrical potential, the orbits have no particular sense of circulation around the center, their time-averaged angular momentum is zero.



## - loop / tube orbits

Look like tubes in a loop.

Viewed on the plane, they look like (elongated) open circular orbits, but they don't stay on a plane. (The tube is three-dimensional.)



See fig.  
38 in  
Binney/  
Tremaine

They can go both around the long or short axis of the ellipsoid.

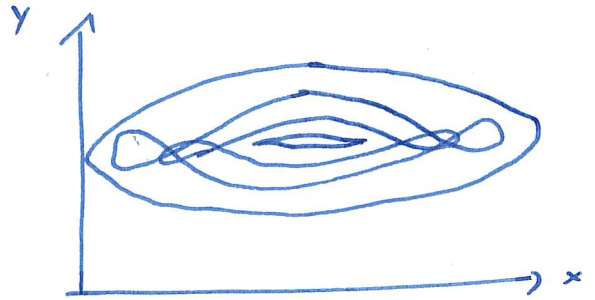
## - chaotic orbits



## Triaxial potentials, rotating

In the core of a rotating potential, the closed orbits are elongated ellipses.

Along the long axis, the closed orbits develop ears.



Note that we solve the problem for triaxial potentials on a plane first, and then just "rotate and scale" the solution to obtain the 3D ellipsoid.

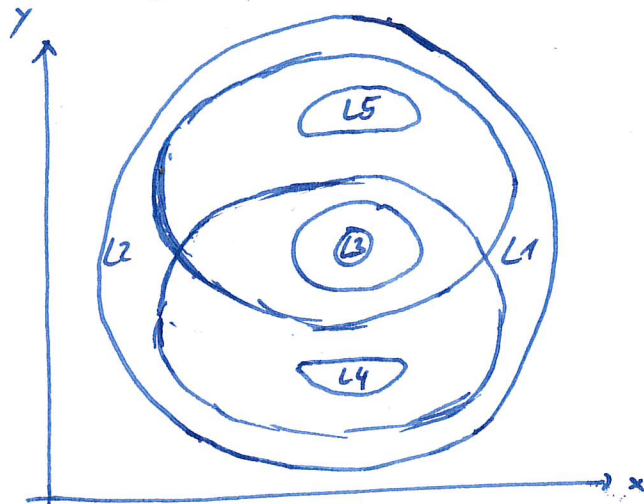
The problem is easier to work with if we set the reference frame to the co-rotating frame. However by moving to a rotating (non-inertial) frame, we introduce a different effective potential. The Hamiltonian of the system is

$$H = \frac{1}{2} (\dot{x}^2 + \dot{y}^2 + \dot{z}^2) + \Phi(x, y, z) - \underbrace{\frac{1}{2} \Omega^2 (x^2 + y^2)}_{\text{centrifugal potential}}$$

We define

$$\Phi_{\text{eff}} = \Phi(x, y, z) - \frac{1}{2} \Omega^2 (x^2 + y^2)$$

This potential has 5 extrema, known as the Lagrange points, where  $\nabla \Phi = 0$ :



L1 & L2: are along the bar, are saddle points. Always unstable.


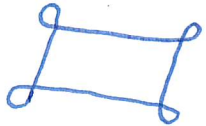
L3: minimum, stable

L4 & L5: are maxima. Stable if the bar is not pronounced.

At each of the L1, L2, L4 and L5 it is possible for a star to travel on a circular orbit while appearing to be stationary in the rotating frame.

How does a bar form in a disk galaxy?

The key to solve this question is to look at (near) periodic (or at least banded) orbits around the center.

Depending on the energy of the star, possible periodic orbits in a triaxial rotating potential are elongated ellipsoids, elongated along the long axis, or even more complex shapes like ears  close to the center or even more complex and also self-intersecting at higher distances: .

There might be some periodic orbits around the Lagrange points, but mostly, we have chaotic orbits.

What about gas, which doesn't behave as stars, which are collisionless?

Gas can flow smoothly if the underlying orbits form a smooth flow in space, which can happen in disks or if a weak bar is present.

For strong bars however, we get self-intersecting orbits. Then, we get shocks. The shock changes the gas phase, and can lead/trigger spiral arms around the bar, identifiable as dust lanes and regions of star formation.

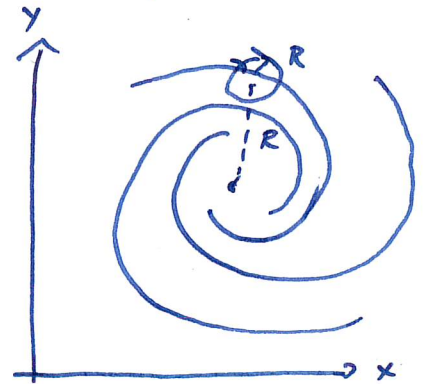


Lastly, we should take a look at resonances.

An orbital resonance occurs in galaxies when an orbit's epicyclic frequency - the frequency of an orbit's radial motion - is a simple multiple of a forcing frequency.

A forcing frequency can be the rate at which an object encounters successive crests of spiral waves or the influence of a rotating central bar.

Compare with the image on the right, where a galaxy is drawn in the rotating frame, and the epicyclic motion of a star at distance  $R$  from the center crosses a spiral multiple times during one period.



The galactocentric distance of a particle that orbits in the equatorial plane of an axisymmetric galaxy is a periodic function of time with period  $T_r$ . During the interval  $T_r$ , the azimuthal angle increases by an amount  $\Delta\phi$  since the orbit doesn't need to be closed over one radial period. The relation between radial and azimuthal frequencies is

$$\Omega_r = \frac{2\pi}{T_r}, \quad \Omega_\phi = \frac{\Delta\phi}{T_r}.$$

In general,  $\frac{\Delta\phi}{2\pi}$  is not a rational number, so the orbit forms a rosette figure.

Now suppose that we view the orbit from a frame that rotates at angular speed  $\Omega_p$ . In this frame, the azimuthal angle is  $\phi_p = \phi - \Omega_p t$ , which increases in one radial period by

$$\Delta\phi_p = \Delta\phi - \Omega_p T_r.$$

Therefore, we can choose  $\Omega_p$  so that the orbit is closed. In particular if  $\Delta\phi_p = 2\pi \frac{m}{n}$ , where  $m$  and  $n$  are integers.

Then:

$$\begin{aligned}\Delta\phi_p &= 2\pi \frac{u}{m} = \Delta\phi - \Omega_p T_r \\ &= \Omega_\varphi T_r - \Omega_p T_r\end{aligned}$$

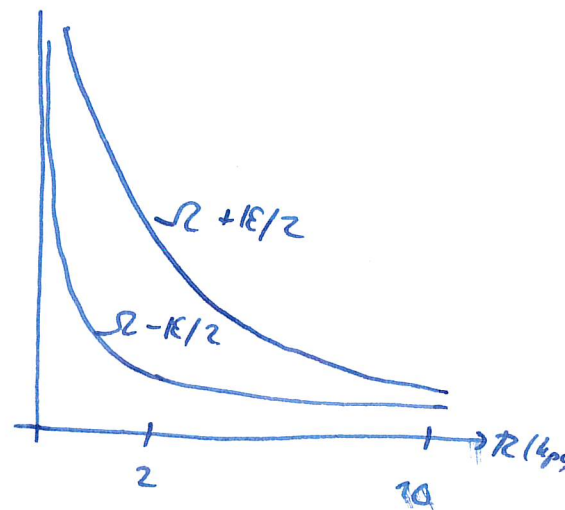
$$\Omega_p = \Omega_\varphi - \frac{2\pi}{T_r} \frac{u}{m} = \Omega_\varphi - \Omega_r \frac{u}{m}$$

$$\approx \Omega - \kappa \frac{u}{m}$$

where  $\Omega$  is the differential rotation for a circular orbit and  $\kappa$  is the epicyclic frequency (the frequency at which a radially displaced particle in a disk will oscillate).

In general,  $\Omega_p = \Omega(R) - \kappa(R) \frac{u}{m}$  is a function of  $R$ , so there is no good/single choice for  $\Omega_p$  that can ensure that orbits at all radii are closed.

While most of the  $\Omega - \frac{\kappa}{m} u$  curves vary rapidly with radius, the curve for  $\frac{u}{m} = \frac{1}{2}$  is relatively constant across much of the galaxy.





Over these (nearly) constant regions, we can actually find a constant rotation for our frame,  $\Omega_p$ , and we can find and place many stars in these regions that will have closed orbits.

If we fill up these orbits with stars, we create a bar-like pattern, which is stationary in the rotating frame and appears as a density wave rotating at the pattern speed  $\Omega_p$  in the inertial frame.

By rotating the axes of the ellipses we can create leading or trailing spiral density waves, which are popular models for the spiral arms of disk galaxies.

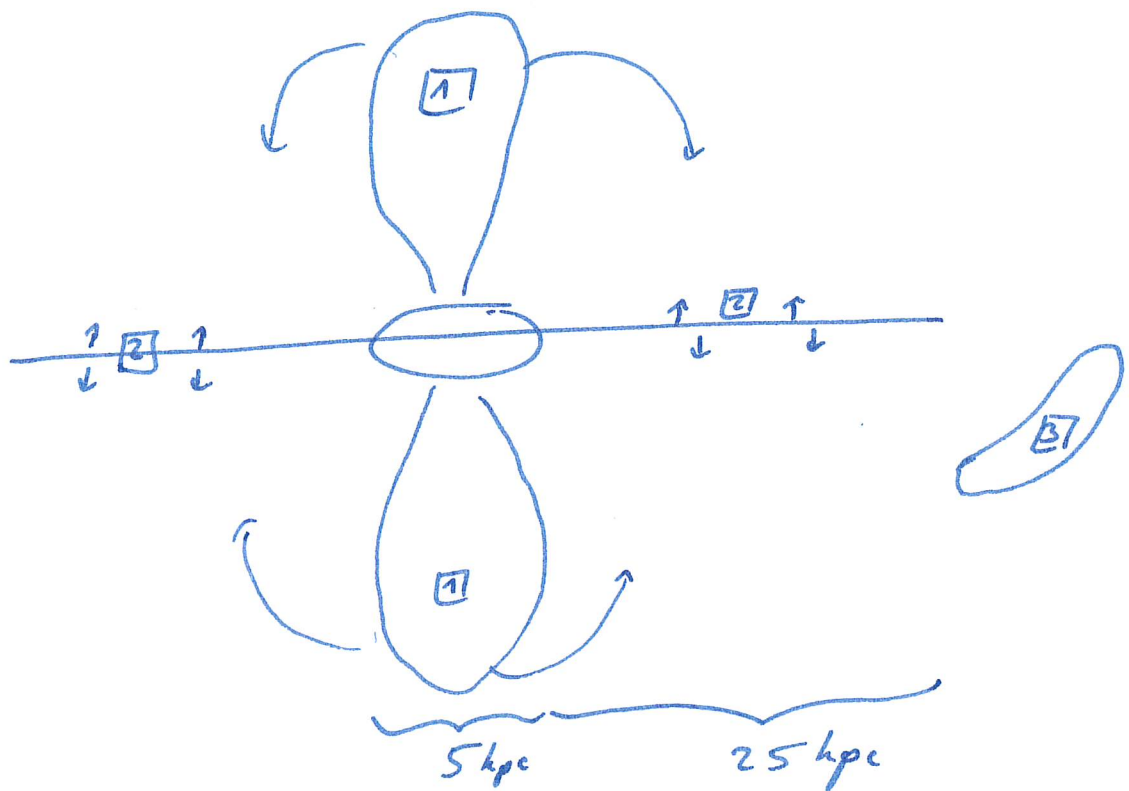
These resonances can also keep up the spiral pattern in the absence of any perturbing force. A weak perturbation will produce a strong reaction which follows the same symmetry.



# The Galactic Halo

The Milky Way has two types of halos:

- A stellar halo, made of stars and diameter  $\sim 50$  kpc
- A massive halo, composed of dark matter



- 1: hot gas bubble, ejected from center with  $T \sim 10^4 - 10^6$  K. The hot gas cools and falls back onto the disk
- 2: Much smaller bubbles and ejecta from SNe in star forming regions
- 3: Sagittarius dwarf spheroidal galaxy; Elongated due to MW's gravitational influence

The (non-dark) halo is composed of multiple things:

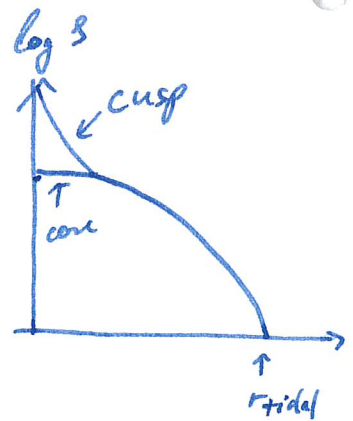
- hot gas  $T \sim 10^4 - 10^6$  K
- stars / stellar halo
- globular clusters: Dense stellar systems orbiting the MW in the halo.  $\sim 150$  identified.
- dwarf spheroidal galaxies: Diffuse stellar clusters which go to larger distances than globular clusters
- dwarf irregular galaxies (Small/Large Magellanic Clouds); Small gas-rich star forming galaxies

# Stellar Halo

- is metal poor  $10^{-2} - 10^{-3} Z_{\odot}$
- $\rho(r) \propto r^{-3.5}$  for  $1 \text{ kpc} \ll r \ll 25 \text{ kpc}$
- $L \approx 4 \cdot 10^7 L_{\odot}$ , indicating small total mass
- $\langle v_{\phi} \rangle \approx -185 \text{ km/s}$  w.r.t. sun: has low rotation in the galaxy frame
- The velocity dispersions hint that the galactic potential is flattened
- average star distribution is  $\sim$  spherical

# Globular Clusters

- There are around 150 globular clusters around the Milky Way, each containing  $10^3 - 10^6$  stars
- Their central density  $\rho_0 \approx 10^4 \text{ M}_\odot / \text{pc}^3$
- Velocity dispersion  $\approx 10 \text{ km/s}$
- Density profile:
  - some clusters have cusps, others have cores
  - they are truncated at a tidal radius



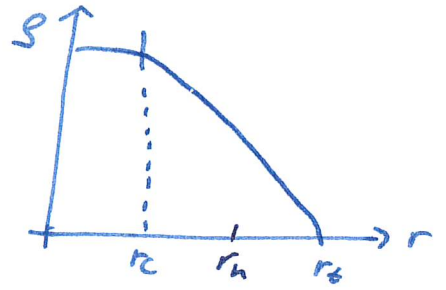
- We can differentiate between two types of clusters based on their spatial distribution:

	"Dish" GC	"Halo" GC
$ z $	$< 3 \text{ kpc}$	$< 20 \text{ kpc}$
$R$	$< 8 \text{ kpc}$	$\leq 40 \text{ kpc}$
$[Fe/H]$	$\geq -0.8$ metal rich	$\leq -0.8$ metal poor
$\langle V_\phi \rangle$ w.r.t. galaxy	$\sim 190 \text{ km/s}$	$43 \text{ km/s}$
$\langle \sigma_{los} \rangle$	$59 \text{ km/s}$	$116 \text{ km/s}$
	rotating GC system w.r.t. galaxy	slowly rotating system



## Properties of Globular Clusters:

- $10^3 - 10^6$  stars
- $\rho \sim 10^4 M_{\odot}/pc^3$
- $\sigma_0 \sim 7 km/s$
- $r_c \sim 1.5 pc$       central radius
- $r_h \sim 10 pc$       half light radius
- $r_t \sim 50 pc$       tidal (truncation) radius
- age:  $\sim 10 - 18$  Gyrs based on stellar models



Clusters exhibit a nearly constant velocity dispersion, which suggests that the relaxation is produced by collective gravitational effects. N-body simulations show that globular clusters, initially in a non-equilibrium state, tend to converge toward virial equilibrium over time.

There are two main relaxation processes:

- violent relaxation:

Happens through collective exchange of particle energies. It's called 'violent' because it's fast compared to the dynamical timescale  $\tau_{\text{dyn}} = \frac{\langle R \rangle}{\langle v \rangle}$ .

- 2-body relaxation:

is characterized by the timescale at which a particle "feels" the effect of the gravitational potential of the other particles in a collisionless system.

The timescale is given by

$$\tau_{2\text{-body}} \approx \tau_{\text{dyn}} \frac{0.1N}{\ln N}$$

where  $N$  is the number of particles in the system.

For globular clusters,  $\tau_{2\text{-body}} \sim$  age of cluster.

The effects of the relaxations are

- mass segregation:

massive stars tend to migrate to the center of the cluster, light stars tend to go to the outer parts (and escape)

- binaries:

binaries form from 3-body interactions and act as a source of "heating":

if a third star approaches a binary, it can gain kinetic energy by interacting with the binaries, leaving them closer to each other and taking the released gravitational energy in and speeding up.

Excess "heat" in light stars helps them escape.

In summary, the total mass of a cluster will shrink over time. After  $\sim 300 t_{\text{dyn}}$ , the total mass may vanish. Binaries are crucial for this mass loss: a single binary can inject kinetic energy into the system

Comparable to the kinetic energy of the entire system.

Tidal interactions with the galaxy aid in the escape of envelope stars. The tidal radius of a globular cluster can be estimated by considering the rotating potential in which the cluster is in. (Think of Lagrange points here.)

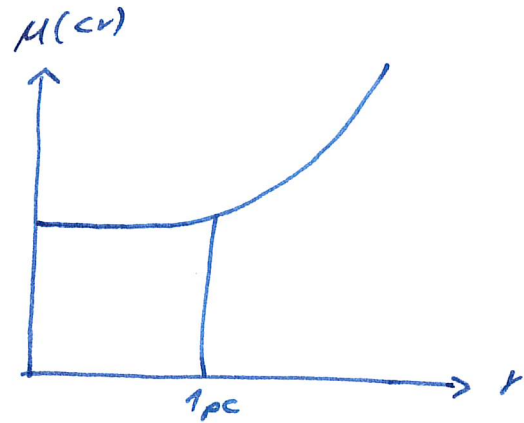
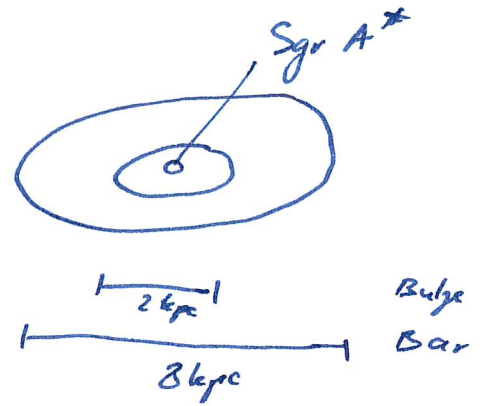
This potential will also strongly influence the shape of the cluster. Most orbits of clusters are elongated, leading to the size of clusters oscillating because the tidal forces change over time.



# Galactic Center

The mass distribution in the galactic center, based on observations, has a plateau very close to the center.

There is a supermassive black hole, Sagittarius A\* with diameter  $6 \times 10^6$  km and mass  $4 \times 10^6 M_{\odot}$  at the center of the galaxy. Sgr A\* is a source of radio emission.



There are  $\sim 10^7$  stars in  $\lesssim 1 \text{ pc}$  of the GC, dominated by red giants. Because of the interstellar dust, the GC can't be studied in visible, UV or X-ray bands  $\Rightarrow$  Radio is important.

Physical processes behind radio emission are accelerated electrons: Brems- or synchrotron-emission via free-free scatterings or present magnetic fields, respectively.

In which wavelengths do we study the GC?

- Near IR ( $\mu\text{m}$ )

stars & dust are barely visible in the GC

- Radio (cm)

- arcs, filaments, SN remnant bubbles, Sgr A\*
- arcs are arc-like structures which are streams running perpendicular to the main filament. (Galactic Center Arc, APOD 080427)
- filaments are radio emission structures like threads. Threads are in isolation and filaments are in bundles and tens of tens of parsecs long. They are uniform in brightness and curvature and in this way they are different from the SN remnants.
- SN remnants: The wrapped gas forms after the explosion of a SN.

- IR (mm) :

dust clouds, cold gas.

From the virial theorem, we can estimate that

$$m(r < 0.001 \text{ pc}) \sim 4 \cdot 10^6 M_{\odot}$$

Stellar cluster distribution around Sgr A\*:

$r \geq 3 \text{ pc}$ : elongated in the galactic plane  
 $r < 3 \text{ pc}$ : spherical distribution





# Groups, Galaxy Clusters and Super-Clusters

- Group of galaxies:  
aggregation of 30 or less galaxies,  
gravitationally bounded
- Cluster of galaxies:  
aggregation of at least 30 galaxies,  
gravitationally bounded, brighter than  
 $m_3 + 2$  where  $m_3$  is the magnitude  
of the third brightest galaxy and  
within a distance of 1-5 Mpc/h from  
the center.

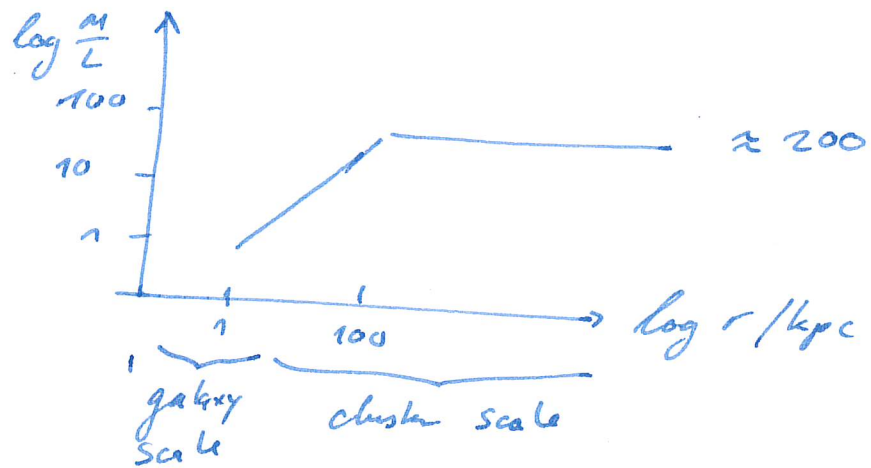
Clusters are the largest virialized structures in the Universe. The richness of a cluster is a measure of the number of galaxies associated with that cluster.

For a cluster with more than 50 galaxies, the overdensity of galaxies is

$$\frac{n_g(\text{cluster})}{n_g(\text{field})} > 200.$$

The mass-to-light ratio for a cluster as a function of the distance to the center is:

is:



There is a threshold: The content of baryons and other kind of mass is bounded

$$\text{by } \Omega = \Omega_{\text{baryons}} + \Omega_{\text{dark}} + \Omega_{\text{r}} = 1$$

Up to some distance, baryons can collapse to form stars and luminosity, but at some point, the cosmological threshold sets in.

## Superclusters:

large group of galaxy clusters or groups; They are the clusters at the intersections of filaments.

### Example:

Milky Way is part of the Local Group

Which is part of the Virgo Cluster

Which is part of the Laniakea Supercluster

### Typical Numbers:

	$N_{gal}$	$R/Mpc$	$V_{los}/km/s$	$M_{dark}$	$\rho/Mpc^{-3}$
Group	3-30	0.1-1	100-500	$3 \cdot 10^{12-14}$	$10^{-3}-10^{-5}$
Cluster	30-300	1-2	400-1400	$10^{14}-2 \cdot 10^{15}$	$10^{-5}-10^{-6}$
Supercl.		150			$10^{-6}$





# Local Group

Size  $\sim 1 \text{ Mpc}$

Association: a set of groups,  $\sim 2 \text{ Mpc}$

Cloud: a set of groups,  $\sim 12 \text{ Mpc}$

Cluster: a set of more than 30 galaxies within  
 $1 \text{ Mpc}$

Beyond clusters, we have that the entire observable universe, which remains similar.

In  $400 \text{ Mpc}$ , we have  $\sim 10^{11}$  galaxies.

The Local Group contains 40 galaxies. The

Milky Way and Andromeda (M31) dominate this gravitationally bound group. The rest of the group is made of dwarfs, many of them are satellites of MW & M31.

In the local group, there are 2 associations and 1 cluster.



# Magellanic Clouds

There are two irregular dwarf galaxies in the local group. They have ongoing star formation, therefore contain both old and young stars.

They are visible in the Southern sky and are called the Large Magellanic Cloud (LMC) and Small Magellanic Cloud (SMC). They are gas rich and metal poor.

The Magellanic stream consists of a series of elongated HI clouds with high velocities that are aligned with each other to form a <sup>swath</sup> (= long band) 21-cm emission that stretches over more than  $60^\circ$  in the southern sky.

This structure is the gas that has escaped from LMC & SMC and now is heating the clouds in their orbit around the MW.

The LMC is classified as a Magellanic spiral. It contains a stellar bar, suggesting that it was a barred dwarf spiral galaxy before its spiral arms were disrupted by tidal interactions from the SMC and MW. Distance: 50 kpc.

The SMC contains a central bar structure which also shows that it was a barred spiral galaxy disrupted by the MW. Distance: 53 kpc.

- HI rotation curves:

The kinematic properties of the HI gas gives information about the mass distribution. The circular velocity ( $v_c$ ) at a given radius is a combination from DM, stars and gas.

HI gas has rotational kinematics in the LMC with the maximum circular velocity  $v_c \sim 60$  km/s. It corresponds to the total mass of  $2.4 \times 10^9 M_\odot$  which can be explained by the mass distribution of the baryonic component (gas and stars) without a dark matter halo for the central 3 kpc.  
 $\Rightarrow$  There is no cusp in the density profile.

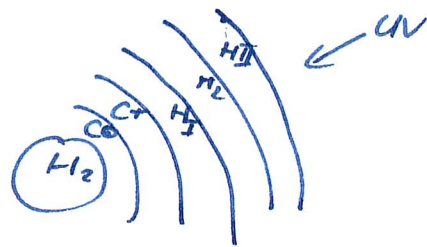


- In mm wavelengths:

$H_2$  is mostly self-shielded.

At high column density,  
 $CO$  is optically thick, but when

$T$  is  $< 20K$ ,  $CO$  is frozen. We can observe  
the rotational transition of  $CO$  even at low  
temperatures  $< 100K$  in cold, dense conditions.

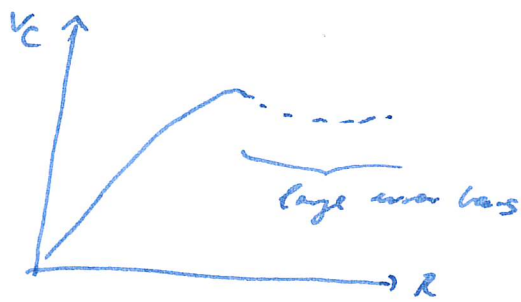


- From  $CO$  emission:

The mass-luminosity relation is higher  
for the LMC than the MW.

The mass of the  $H_2$  cloud is obtained  
by the virial theorem and the velocity  
dispersion in the cloud.

- Information from the 21-cm line (HI line)  
 magnetic clouds have a bar structure in the  
 inner region. From the rotational motion we  
 can get the mass distribution:



$$v_c^2 = \frac{GM}{r} \quad \text{with} \quad \frac{M}{L} = 1.8$$

Masses for LMC:  $R < 4 \text{ kpc}$

$$\begin{aligned} * &= 1.4 \cdot 10^9 M_{\odot} \\ \text{gas} &= 0.4 \cdot 10^9 M_{\odot} \\ \text{DM} &= 1.0 \cdot 10^9 M_{\odot} \end{aligned}$$

The rotation curve is measured through the  
 doppler shift of the 21cm line spectra.

The assumption is that 21 cm emission is  
 emitted isotropically and thus traces the motion.

The velocity dispersion can be measured by the  
 width of the emission line.

# Laniakea Supercluster

Contains  $\sim 10^5$  galaxies.

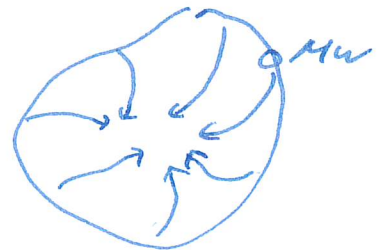
To get the flow lines of galaxies or groups in a supercluster, you need eigenvalues and eigenvectors of the shear tensor. The Eigenvalues give the velocities and the Eigenvectors give the direction of motion.

Let  $\langle \vec{v} \rangle$  be the average velocity of a group in a super cluster. Then the shear tensor

is

$$\begin{pmatrix} \frac{\partial \langle v \rangle_x}{\partial x} & \frac{\partial \langle v \rangle_y}{\partial x} & \frac{\partial \langle v \rangle_z}{\partial x} \\ \frac{\partial \langle v \rangle_x}{\partial y} & \dots & \vdots \\ \dots & \dots & \dots \end{pmatrix}$$

The flow lines look something like this:



The MW is almost at the border of the Laniakea Supercluster.

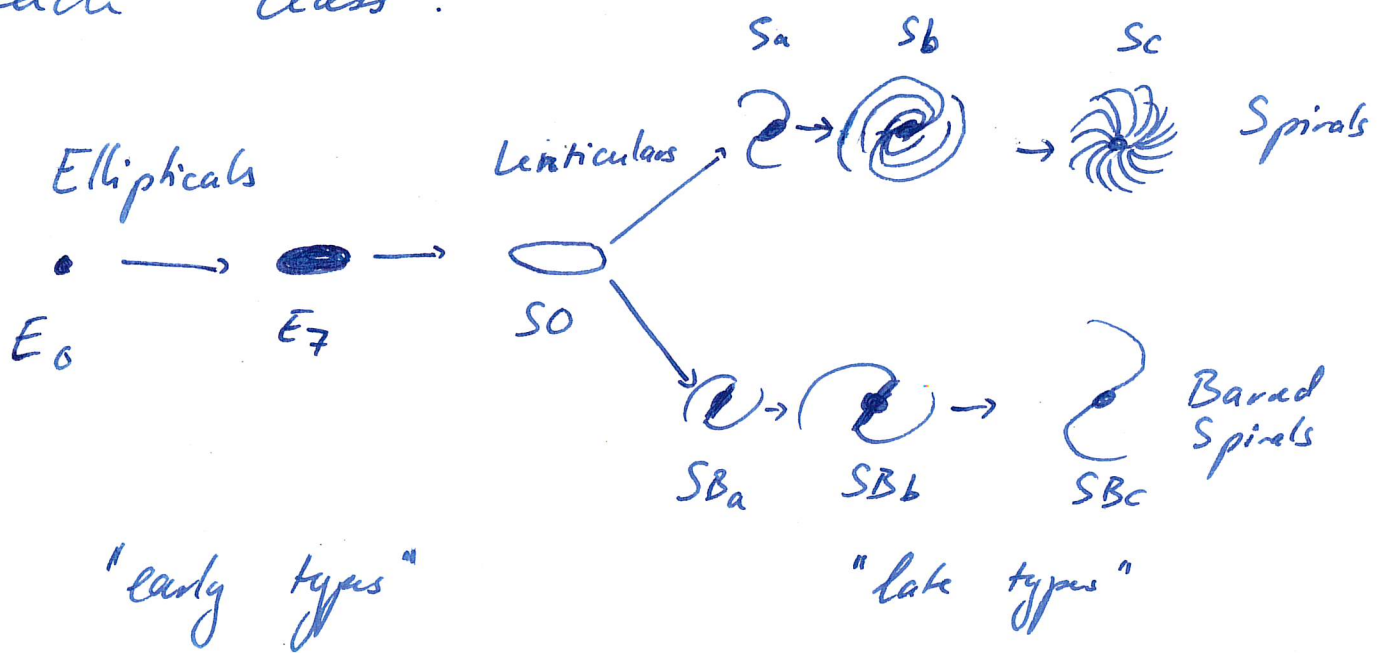
Beyond 100 Mpc, homogeneity starts to hold.  
At these scales, the average density should  
remain  $\sim$  constant.



# Hubble Sequence Correlations

## Hubble Sequence

The Hubble Sequence is a morphological classification for galaxies. It is based on their appearance in the optical band and assigns a label corresponding to each "class".



- Ellipticals are characterized by their eccentricity:  
 $E_n$  where  $n = 10(1 - \frac{b}{a})$
- Lenticulars:  $SO/SBO$  have a bulge and a disk (and possibly a bar) but no arms

- Spirals: have spirals in their disk.  
Classified according to how tightly wound the spirals are and how bright the bulge is. Both quantities decrease while moving to the right.

Sd added by De Vaucouleurs: very loosely wound, fragmentary arms, most of the luminosity is in the arms and not the bulge.

- Irregulars: Do not fit on the tuning fork, are asymmetric

# Extended Classifications

- de Vaucouleurs' classification:

retains Hubble's basic division into ellipticals, lenticulars, spirals and irregulars. Introduced a more elaborate classification system for spirals based on 3 characteristics:

- Bars: SB for bars, SA for no bars

- Rings: r with rings, s without

- Spiral arms:

- added Sd: diffuse, broken arms made up of individual clusters and nebulae. Very faint central bulge.

- added Sm: irregular, no bulge

- Im: Highly irregular galaxy

- The Hubble stage T:

Assigns a number to Hubble stages ranging from -6 to 10

- David Dunlap Observatory classification:

Add a number I-V by decreasing luminosity to Sa → Sc types.

I refers to supergiant galaxies, V to dwarf galaxies.

- Yerkes classification: Based on spectra instead of galaxy shapes.



# Galaxy Properties and Morphology

The Hubble classification succeeds also in separating galaxies according to their physical and kinematic properties.

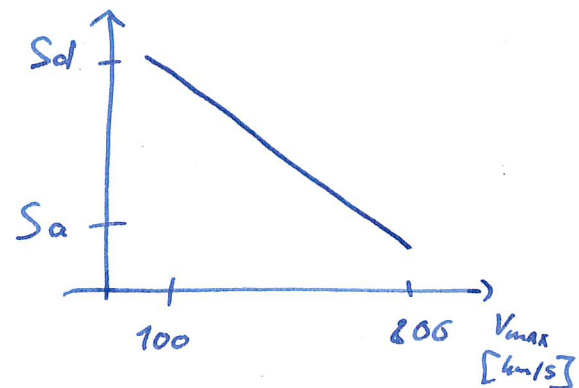
For spiral types:

- Total energy:

From virial theorem:  $E_{tot} \propto -E_{kin}$

$E_{kin}$  is easier to measure.

From observations, we have that  $v_{max}$  increases, implying that the  $E_{kin}$  increases.



- Bulge size:

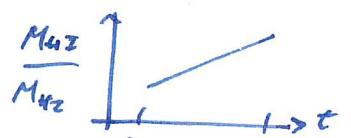
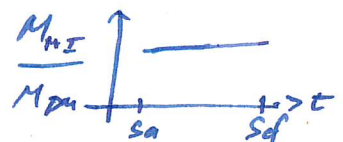
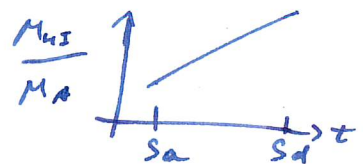
$Sa \rightarrow Sc$ : Bulge fraction decreases

- Mass ratios:

$$\bullet \log_{10} \frac{M_{HI}}{M_{*}} = 0.178t - 1.7$$

$$\bullet \log_{10} \frac{M_{HI}}{M_{DM}} = 0.048t - 1.58$$

$$\bullet \log_{10} \frac{M_{HI}}{M_{H2}} = 0.163t - 0.765$$

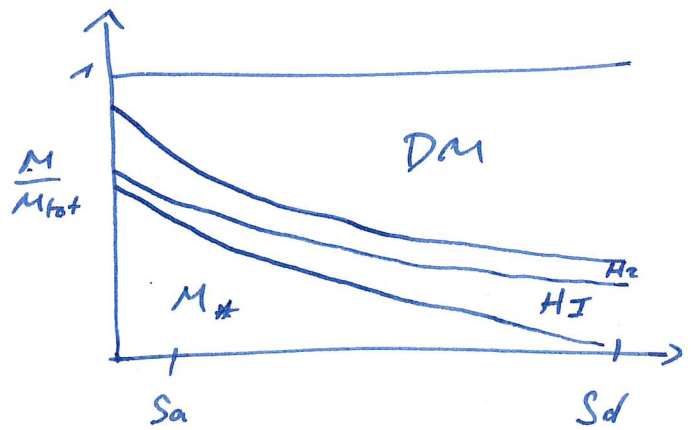
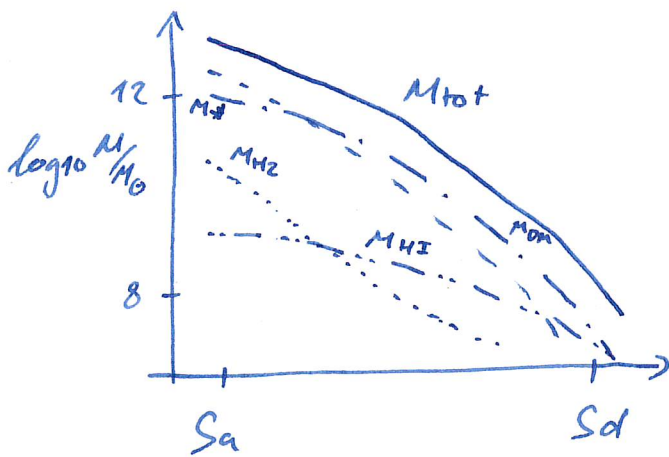


⇒ The ISM of an early-type spiral tend to be more molecular, while late-type spirals tend to be more atomic

We can estimate the total mass as

$$M = M_{\star} + M_{DM} + M_{HI} + M_{H_2}$$

and resolve for each ratio:



### Late Types

More atomic H

Less stars than gas

### Early types

More molecular H

More stars than gas

- Metal fractions:

Sa  $\rightarrow$  Sd:  $\frac{O}{H}$  decreases

This is an irreversible process!

Since late type galaxies have more gas and less stars and the metallicity increases, this suggests that galaxy aging goes from late to early types: Sd  $\rightarrow$  Sc  $\rightarrow$  Sb ...

There is however a problem: There is not enough gas available in late-type galaxies to produce early type star abundances.

- Present star formation rate:

Sa  $\rightarrow$  Sd: SFR increases, which is consistent with "galaxy aging" early  $\rightarrow$  late types.

However, the transformation of gas into stars is an irreversible process. The typical timescale to consume all the gas at the present observed rates is  $\sim 10^9$  yrs, which is much smaller than the galaxy age!

# Faber-Jackson Relation

The Faber-Jackson relation is an empirical power-law between the luminosity and the velocity dispersion of elliptical galaxies:

$$L \propto \sigma^4$$

However, this relation has quite poor correlation. (A study gives  $L \propto \sigma^2$  for low-luminosity ellipticals and  $L \propto \sigma^5$  for very luminous ones.)

From theory, we estimate using the virial theorem:

$$2K + U = 0 \Rightarrow 2 \cdot \frac{1}{2} M \langle v^2 \rangle + - \frac{GM^2}{R} = 0 \Rightarrow M = \frac{\langle v^2 \rangle R}{G}$$

We can write:

$$L = \frac{M}{M_{\odot}} = \frac{L}{M} \frac{\langle v^2 \rangle R}{G} \propto \langle v^2 \rangle R$$

$\sim \text{const}; L \propto M$

So we have 3 parameters ( $L, \langle v^2 \rangle, R$ ) and we can fit a fundamental plane through these observables:  $L \propto \sigma^u R^m$

where empirically  $u \approx 2$  and  $m \approx 1$ , close to virial theorem predictions.



## Tully - Fisher Relation

The Tully - Fisher relation is an empirical correlation between luminosity and rotation velocity of spiral galaxies:

$$L \propto v_{\text{rot}}^n$$

The power  $n$  depends of the colour used to measure the luminosity:

blue, present SFR  $3 \leq n \leq 5$  red, NIR no SFR

$\Rightarrow$  The brighter a spiral is, the faster it rotates

Other forms of the TF relation exist, as the baryonic Tully - Fisher: luminosity is replaced by total baryonic mass:

$$M_{\text{baryon}} \propto v_{\text{rot}}^n, \text{ where } n \approx 4$$

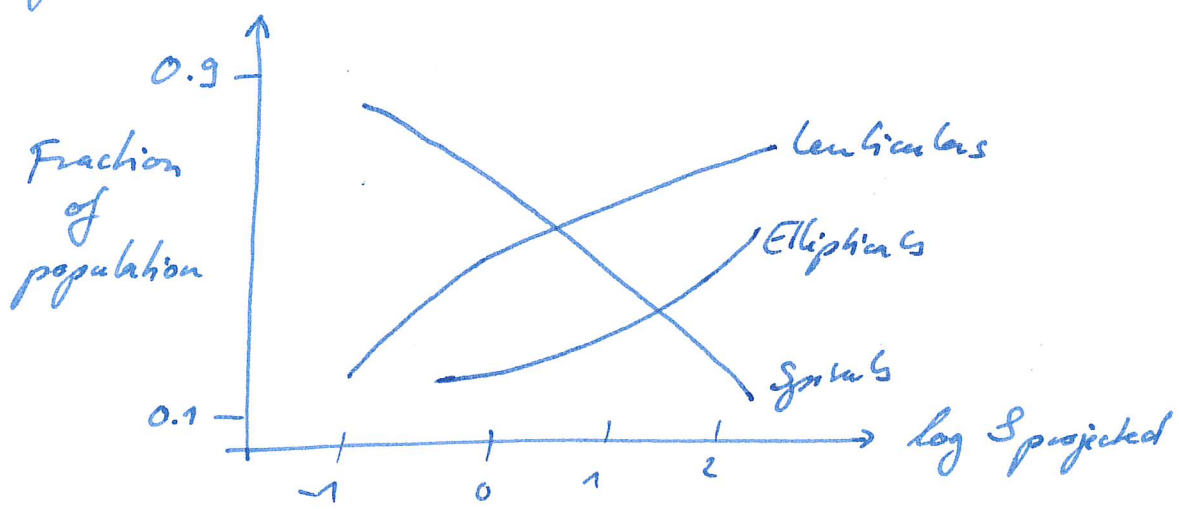
$$\text{and } M_{\text{baryon}} = M_{\text{star}} + M_{\text{HI}} + M_{\text{H}_2}$$

This law gives a better correlation.

# Morphology - Density Relation

The morphology - density relation is an empirical relationship between the Hubble types of galaxies and the environments in which they are located.

There is a correlation between the density of galaxies and their morphology:



$S_{\text{projected}}$ : the galaxy density projected on the observed surface, i.e. density integrated along LoS.

- Early type galaxies (SO, E) are preferentially located in high density environments
- Late type galaxies are preferentially located in low density environments
- In clusters, E and SO galaxies are common, and spirals are rare

Inside a cluster, a population gradient as a function of distance exists.

From the center of the cluster:

- Ellipticals occur mainly near the center
- Spirals predominate in outer regions

These observations indicate that galaxy evolution is affected by the environment in which the galaxy is. It is explained by different aspects:

- The galaxies' motion through the intergalactic medium in a cluster at a speed  $\sim 1000$  km/s causes shocks/interactions between colder gas in the galaxies and the hot gas in the medium. So it strips/removes the galaxy gas, which will change the morphology  $\Rightarrow$  lenticulars. This effect is called ram pressure.



- As galaxies enter the cluster environment for the first time, the gravitational potential of the cluster create tidal effects that enable the gas contained within the galaxy to escape. Again it will change its morphology ( $\Rightarrow$  lenticular). As the gas is lost in the intra-cluster medium, the amount of gas available to produce stars decreases, and star formation will cease. This effect is called galaxy strangulation, or harassment when this is not the whole cluster but a few galaxies which produce tidal effects.

- Mergers of galaxies result generally in ellipticals.

All of this leads to:

- spirals don't survive ~~to~~ a single crossing through the cluster.
- transformations of galaxies (aging) goes from  $S \rightarrow SO \rightarrow E$



# Galaxy Luminosity

The luminosity function gives the number of galaxies per luminosity interval.

The Schechter luminosity function is a parametric description of the density of galaxies as a function of their luminosity.

$$\phi(L) = \frac{\phi^*}{L^*} \left(\frac{L}{L^*}\right)^\alpha e^{-L/L^*}$$

where  $\phi^*$ ,  $L^*$ ,  $\alpha$  are fitting parameters.

$\alpha$  is the slope of  $\phi$  at low  $L$

$\phi^*$  is the reference density of galaxies

$L^*$  is the characteristic luminosity.

$\phi(L)$  can be converted to  $\phi(M)$ , where  $M$  is the magnitude, using  $M = -2.5 \log L$

The total number of galaxies is

$$\int_0^{\infty} \phi(L) dL$$

The total light is

$$\int_0^{\infty} L \phi(L) dL = \phi^* L^* \Gamma(2+\alpha)$$

In fact,  $\alpha$  depends quite poorly on colour and more strongly on  $M^*$

For field galaxies

$$\alpha \sim -1$$

$$L^* \sim 1.2 h^{-2} 10^{10} L_{\odot}$$

$$\phi^* \sim 1.6 h^3 10^{-2} \text{Mpc}^{-3}$$

cluster galaxies

$$\alpha \sim -1.27$$

$$M^* \sim -19.5$$



typical luminosity function

## Light Profile

Let  $I(r)$  be the intensity per unit surface as a function of distance  $r$ .

Let  $\mu$  be the surface magnitude for elliptical and spiral galaxies.

Ellipticals:

$$\mu = \log \frac{I(r)}{I(r_e)} = -3.3307 \left[ \left( \frac{r}{r_e} \right)^{1/4} - 1 \right]$$

$r_e$ : half light radius

Spirals:

$$\mu = \log \frac{I(r)}{I(r_s)} = -\frac{r}{h}$$

$h$ : characteristic length of the disk

For the bulge, we have the Sérsic law which says that the Bulge is sometimes like an elliptical and sometimes like a spiral:

$$\mu = \log \frac{I(r)}{I(r_0)} = - \left( \frac{r}{r_0} \right)^{1/u}, \quad u \in (1, 4)$$



# Galaxy Interactions

Generally, we can distinguish between two types of galaxy-galaxy interactions:

- accretion, where  $m_1 \gg m_2$
- merger, where  $m_1 \approx m_2$

These interactions can be modelled on different levels:

- As 2-body interactions:

Approximate both galaxies as point masses. Energy, momentum, angular momentum and masses are conserved.

There is no special phenomenon associated to this type of interaction.

- As restricted 3-body problem:

Represent both galaxies with a central particle each, containing the entire mass, and each surrounded by many massless particles, moving freely in the present potential.

No merging takes place in this kind of model for the interaction, but the 'galaxies' already develop tidal tails and bridges (matter 'bridge' between the two galaxies after the interaction.)

- As an  $N$ -body problem

Represent the galaxies as a group of particles (commonly all particles have equal masses.)

These kinds of interactions reveal merging events as well as internal spiral and density waves in the disk.

$N$ -body models can be quite expensive to compute. A direct force computation of a simulation with  $N$  particles will require  $\frac{N(N-1)}{2}$  interactions per timestep, each interaction requiring  $\mathcal{O}(100)$  floating point operations. So this computation scales with  $\mathcal{O}(N^2)$ .

Instead, various approximations have been introduced. The most commonly adapted techniques are spectral or tree methods, or combinations of them.

- Spectral methods solve the Poisson equation in Fourier space, where the  $\nabla^2 \phi$  transforms to  $-k^2 \tilde{\phi}$ , a simple multiplication, and using the Fast Fourier Transform.
- Tree codes (recursively) group particles close to each other in cells. For other very close particles, the direct force



computation is used. For groups of particles sufficiently far away, the gravitational force is computed using a multipole/Taylor expansion. It turns out that the different terms of the expansion can be written as a function of distance to the particle for which they are computed only, while the other parts of the components can be pre-computed for every group. (So you need to compute the multipoles only once for each group, regardless on which particle you want them to act on.)

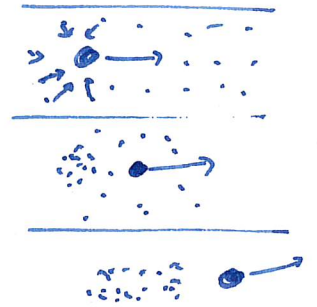
- As full hydrodynamics & gravity simulations:  
Many more effects are incorporated when hydrodynamics for baryons come into play. These include shocks and singularities, cooling, star formation, radiation, heating, cosmic rays, metals, stellar and supernova feedback...



Note that in  $N$ -body models, only gravity is treated; So how exactly do these galaxies merge when there is no model for particle collisions included?

→ the answer is dynamical friction.

Consider a mass travelling through a collisionless group of particles. The mass will at any time  $t$  attract the other



particles towards its current position. At a later time  $t + \Delta t$ , the mass will have moved away, but the other particles will have moved towards its previous position, creating an overdensity at that position.

This overdensity's gravitational influence, which will always be directly behind the mass, will act to slow the mass down.

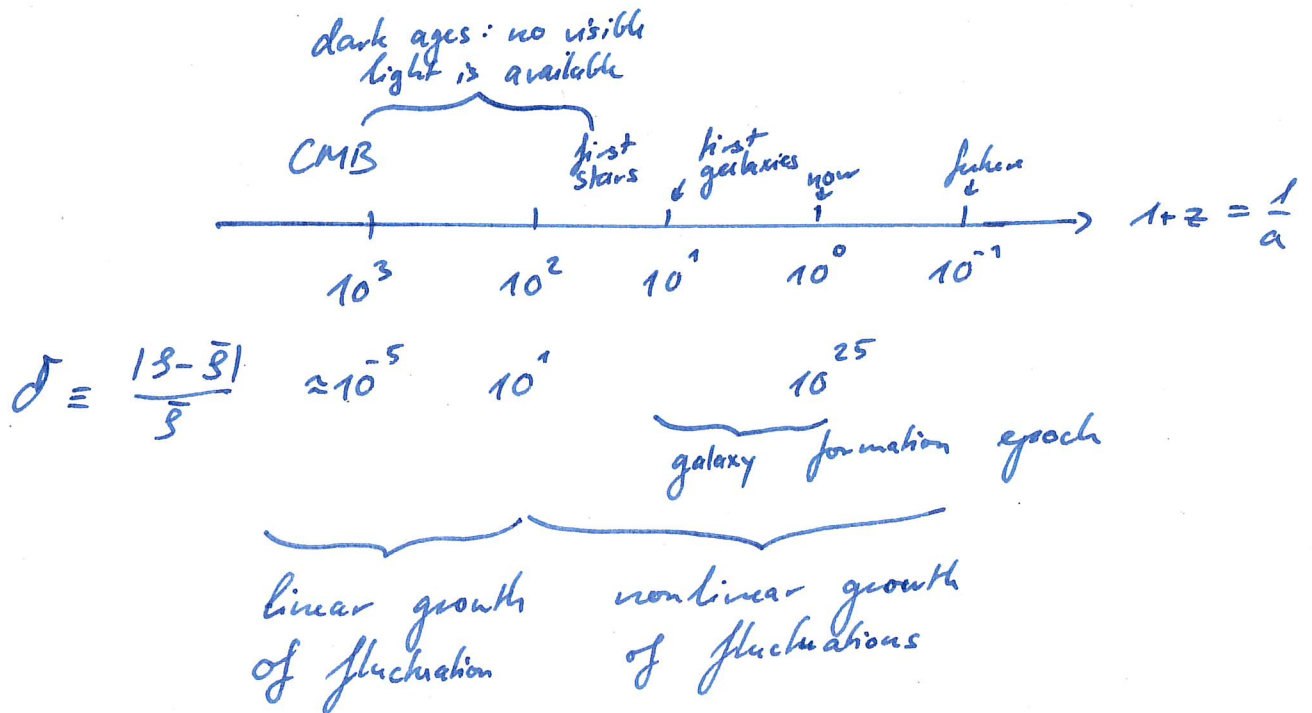
Now suppose the position of this mass is in the outer disk part of a

galaxy that is modelled like this using collisionless particles. The mass will move according to the galaxy's potential, but slowly lose kinetic energy over time due to dynamical friction, and eventually fall into the big galaxy's center and stay there.

Another effect is tidal stripping: the tidal forces of the big galaxy's potential can be quite violent inside the galaxy's disk, so if instead of a point mass we consider another, smaller, galaxy falling into a big one, over time it will be stripped away of its particles starting at the outer layers, thus losing mass, thus losing energy.

# Galaxy and Structure Formation

Since the Big Bang, we can differentiate between two regimes of structure formation:



In the linear regime of fluctuation growth, the theory available can explain a lot. In the nonlinear regime however, there is no good theory available, and we must rely on computer simulations to make advances. How terrible! :)



In the old view of structure formation, it was assumed that galaxies form through fast collapses that set in because of gravitational instabilities. (Think Jeans mass, spherical collapse, just like star formation, but bigger.) This would imply that the formation time of galaxies is relatively fast and characterized by the free-fall time of  $\sim 10^7$  yrs. It also implies that once formed, the galaxy morphology would remain frozen.

In the present view, one doesn't assume a spherical, but an elliptical collapse, assuming a density in an ellipsoid with axes  $a, b, c$

$$S(t) = \bar{S} \frac{R^3(t)}{(R(t) - \alpha g(t))(R - \beta g)(R - \gamma g)}$$

where  $\alpha, \beta, \gamma < 0$  are constants depending on  $a, b, c$  and  $R(t), g(t)$  depend on time via the cosmological model which determines the expansion



As can be easily seen, this density  
can encounter singularities over time, when

$$\begin{aligned} \alpha g(\epsilon) &\sim R(\epsilon) && \text{and/or} && \text{"sheet singularity"} \\ \beta g(\epsilon) &\sim R(\epsilon) && \text{and/or} && \text{"filament singularity"} \\ \gamma g(\epsilon) &\sim R(\epsilon) && && \text{"point singularity"} \end{aligned}$$

If such a singularity occurs, it triggers  
a cascade of smaller collapses. This is a  
hierarchical process, it happens at smaller  
scales recursively.

Large structures are then formed through  
a series of merging events (dominant process)  
and accretion of surrounding mass.

# Structure Formation Timescales

For structure to form, the medium needs to collapse, but also to cool sufficiently. Otherwise, the heat will prevent the collapse.

We can estimate the collapse timescale as the free-fall time:

$$\tau_{\text{ff}} \sim \frac{1}{\sqrt{G\rho}} \propto \frac{1}{\sqrt{n}} \quad n: \text{ number density}$$

and the cooling with the cooling timescale:

$$\tau_{\text{cool}} = \frac{E}{\left| \frac{dE}{dt} \right|} \propto \frac{3nkT}{n^2 \Lambda(T)}$$

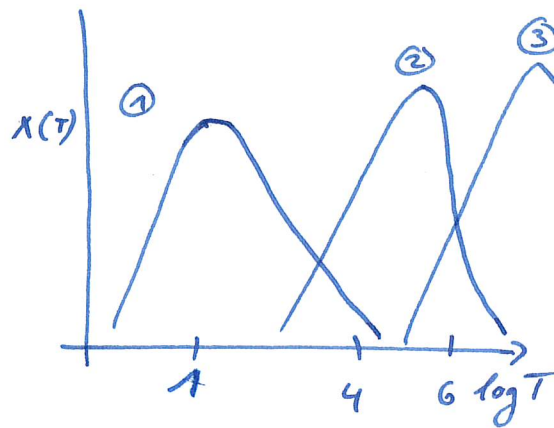
where  $\Lambda(T)$  is the cooling function.

For a collapse, we then have the condition

$$\tau_{\text{cool}} < \tau_{\text{ff}}$$

which effectively limits the the possible galaxy mass range.

There are 3 typical "peaks" of the cooling function  $\Lambda(T)$  at different temperatures, corresponding to different excitations:



① At  $\sim 10-100$  K, rotational levels of molecules and fine-structure levels of atoms begin to be excited by collisional impacts.

② At  $\sim 10^4$  K, enough particles in the distribution have sufficient energies to collisionally excite the lower-lying electronic states of the common elements like H and He.

③ At  $\sim 10^6$  K, the inner shells of elements like O and Fe can be excited.

In general, the presence of metals increases the cooling function at all temperatures by providing new/more possible excitation states which can radiate away energy from the medium.

